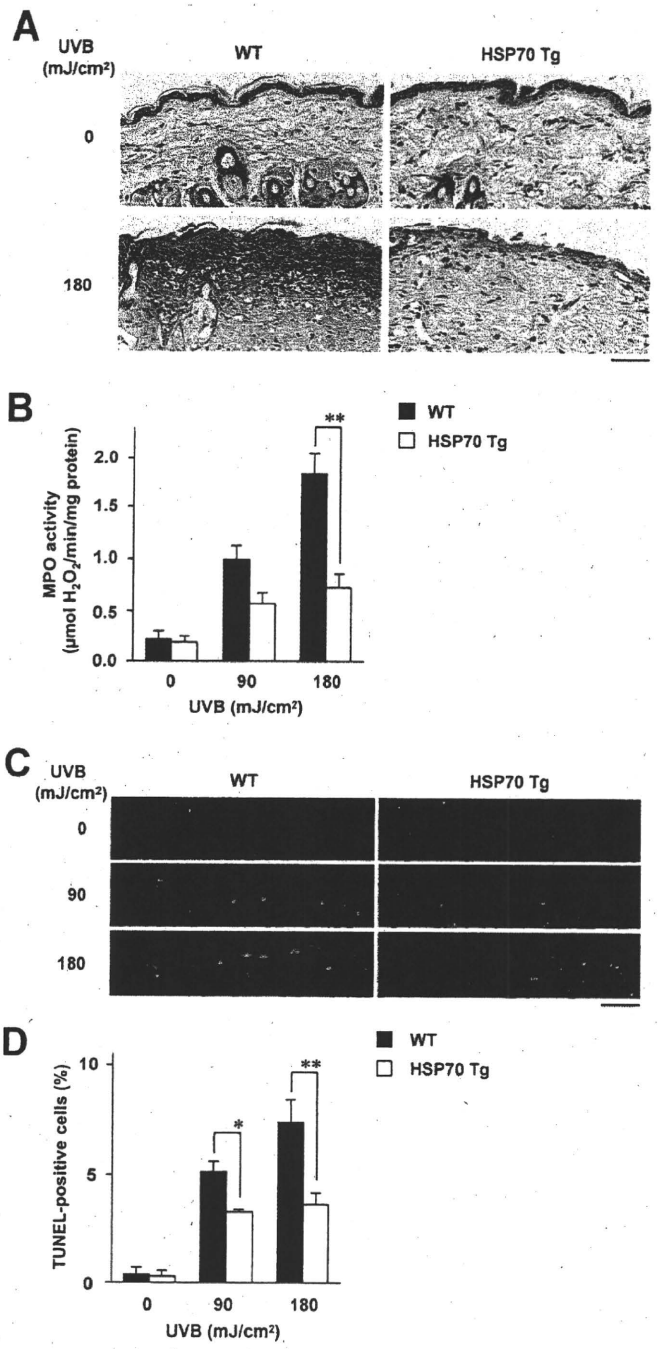

FIGURE 2. **UVB-induced skin damage and apoptosis in wild-type mice and transgenic mice expressing HSP70.** Transgenic mice expressing HSP70 (*HSP70 Tg*) and wild-type mice (*WT*) were irradiated with or without the indicated doses of UVB, and the dorsal skin was removed after 48 h (*A*), 24 h (*B*), or 12 h (*C* and *D*). *A*, sections of dorsal skin were prepared and subjected to hematoxylin and eosin staining. *B*, MPO activity was measured as described under "Experimental Procedures." Values are mean ± S.E. ($n = 8-12$). **, $p < 0.01$. *C*, sections of dorsal skin were subjected to TUNEL assay and DAPI staining. *D*, the ratio of TUNEL-positive cells in the epidermis was counted (400–1000 cells in total). Values are mean ± S.E. ($n = 3$). **, $p < 0.01$; *, $p < 0.05$. *Scale bar*, 50 μm.

results suggest that the transgenic mice and wild-type mice irradiated with UVB express HSP70 in various types of cells at the skin.

We also tried to examine the effect of expression of HSP70 induced by geranylgeranylacetone (GGA), a leading anti-ulcer drug on the Japanese market and an HSP inducer (41). However, as shown in supplemental Fig. S3, GGA did not induce expression of HSP70 by any route of administration (oral, intraperitoneal, and percutaneous administrations). Thus, we used heat treatment to induce expression of HSP70. As shown in supplemental Figs. S3 and S4, heat treatment induced the expression of HSP70 at the skin, and we found that this heat treatment protects the skin from UVB-induced damage (epidermal disruption, increase in MPO activity, and epidermal apoptosis).

To test the idea that the expression of HSP70 protects epidermal cells (keratinocytes) from UVB-induced apoptosis *in vitro*, we constructed a stable transfection of a mouse keratinocyte cell line (PAM212) that continuously overexpresses HSP70 (Clone 2). As shown in Fig. 3*A*, the level of HSP70 in Clone 2 was higher than mock transfectant control cells in both the presence and absence of UVB irradiation. We also found that UVB irradiation up-regulated the expression of HSP70 in both types of cells (Fig. 3*A*). Exposure of cells to UVB irradiation decreased cell viability in a dose-dependent manner; this effect was suppressed in HSP70-overexpressing cells (Fig. 3*B*). To detect UVB-induced apoptosis, we counted cells in sub-G_1 (apoptotic cells) by fluorescence-activated cell sorting analysis. UVB irradiation increased the number of apoptotic cells, and this increase was suppressed in HSP70-overexpressing cells (Table 1). We also monitored apoptosis by measuring caspase-3-like activity using fluorogenic peptide substrates and obtained similar results to those for the fluorescence-activated cell sorting analysis (Table 1). Overexpression of HSP70 did not affect the background level of apoptosis (Table 1). The results in Fig. 3 and Table 1 suggest that the expression of HSP70 helps to protect keratinocytes from UVB-induced apoptosis.

Effect of HSP70 Expression on UVB-induced Epidermal Inflammation—As described above, HSP70 was reported to suppress the activation of NF-κB through various mechanisms such as suppression of the inflammatory stimuli-induced degradation of IκB-α (an inhibitor of NF-κB) (26). We therefore examined the effect of UVB irradiation and/or expression of HSP70 on the level of IκB-α both *in vivo* and *in vitro*. As shown in Fig. 4 (*A* and *B*), UVB irradiation decreased the cutaneous level of IκB-α both in wild-type mice and in transgenic mice expressing HSP70, although the level remained significantly higher in the latter. We also compared the mRNA expression of pro-inflammatory cytokines (IL-1β and IL-6) and chemokines (MIP-2 and MCP-1) between UVB-irradiated transgenic mice expressing HSP70 and wild-type mice. The mRNA expression of *il-1β*, *il-6*, *mip-2*, and *mcp-1* was increased by UVB irradiation, but this increase was much lower in skin samples prepared from transgenic mice expressing HSP70 compared with samples from wild-type mice (Table 2*A*). The expression of HSP70 in transgenic mice did not affect the background levels of mRNA expression (Table 2*A*). Similar results were observed for the protein levels of cytokines (IL-1β and IL-6) determined by enzyme-linked immunosorbent assay (Table 2*B*). The results in Fig. 4 and Table 2 suggest that expression of HSP70 in the skin suppresses the UVB-induced expression of cytokines and chemokines via the inhibition of IκB-α degradation and the resulting suppression of NF-κB activity.

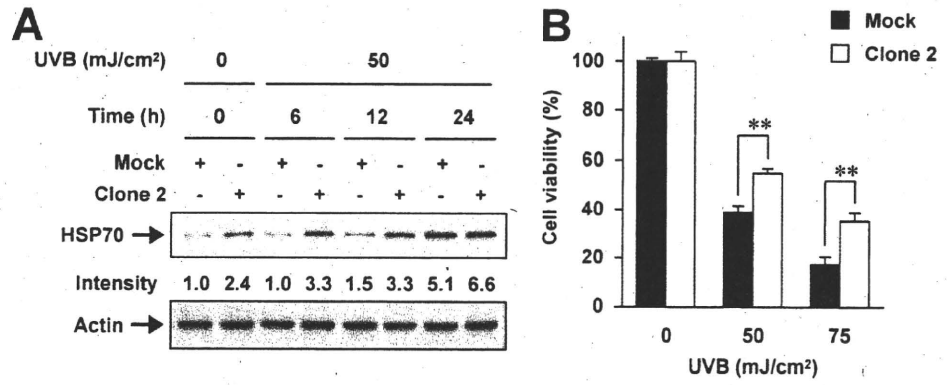

FIGURE 3. **Effect of HSP70 expression on UVB-induced apoptosis *in vitro*.** HSP70-overexpressing PAM212 cells (*Clone 2*) and mock transfectant control cells (*Mock*) were irradiated with or without indicated doses of UVB and cultured for indicated periods (*A*) or 24 h (*B*). *A*, whole cell extracts were subjected to immunoblotting with an antibody against HSP70 or actin. The relative HSP70 band intensity is shown *under the band*. *B*, cell viability was determined by the MTT method. Values are mean ± S.E. ($n = 3$). **, $p < 0.01$.

TABLE 1

Effect of HSP70 expression on UVB-induced apoptosis *in vitro*

HSP70-overexpressing PAM212 cells (Clone 2 in Fig. 3) and mock transfectant control cells (Mock) were irradiated with or without indicated doses of UVB and cultured for 24 h. Apoptotic cells (cells in sub-G_1) were counted by fluorescence-activated cell sorting. Caspase-3-like activity was measured. Values are mean ± S.E. ($n = 3$).

UVB	Cells in sub-G_1		Caspase-3-like activity	
	Mock	Clone 2	Mock	Clone 2
mJ/cm²	%		*Units/mg protein*	
0	2.8 ± 0.37	1.6 ± 0.24	14.2 ± 2.5	27.6 ± 5.7
50	19.2 ± 0.26	10.3 ± 0.18[a]	762.9 ± 19.0	601.7 ± 29.3[a]
75	65.2 ± 1.40	24.4 ± 0.28[a]	1316.9 ± 7.4	700.7 ± 12.6[a]

[a] $p < 0.01$.

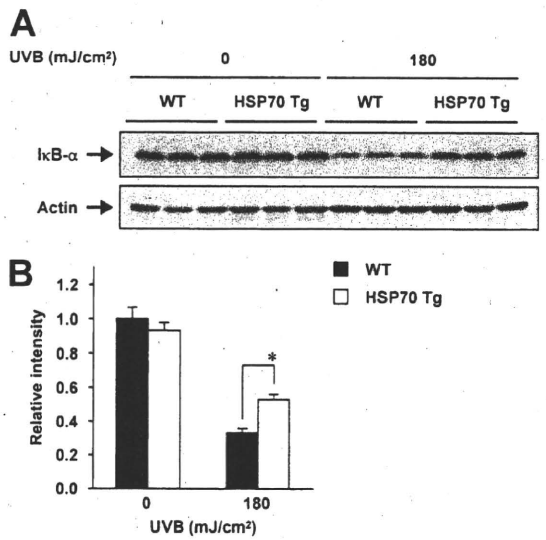

FIGURE 4. **UVB-induced decrease in the level of IκB-α.** Transgenic mice expressing HSP70 (*HSP70 Tg*) and wild-type mice (*WT*) were irradiated with or without 180 mJ/cm² UVB. *A*, the dorsal skin was removed after 48 h, and whole cell extracts were analyzed by immunoblotting with an antibody against IκB-α or actin. *B*, the band intensity of IκB-α was determined and expressed relative to the control sample (one of two gels is shown in *panel A*). Values are mean ± S.E. ($n = 6$). *, $p < 0.05$.

To test this notion *in vitro*, we examined the effect of UVB irradiation and/or expression of HSP70 in cultured keratinocytes on the degradation of IκB-α and expression of just one pro-inflammatory cytokine (IL-6, it has been reported that IL-1β is not expressed in mouse keratinocytes (42, 43)) and chemokines (MIP-2 and MCP-1). As shown in Fig. 5*A*, UVB irradiation transiently (at 6–12 h after the UVB irradiation) decreased the level of IκB-α, and this level was higher in HSP70-overexpressing cells than in mock transfectant control cells at any period after the UVB irradiation. Expression of HSP70 increased the background level of IκB-α (Fig. 5*A*), these results being different from those observed *in vivo* (Fig. 4*A*). Furthermore, expression of the pro-inflammatory cytokine and chemokine genes tested (*il-6*, *mip-2*, and *mcp-1*) was up-regulated by the UVB irradiation, although the expression was suppressed in UVB-irradiated HSP70-overexpressing cells compared with mock transfectant control cells (Fig. 5*B*). Overexpression of HSP70 suppressed the background expression of *mcp-1* but not *il-6* and *mip-2* genes (Fig. 5*B*). The results in Fig. 5 support the notion that the expression of HSP70 in keratinocytes suppresses the UVB-induced expression of cytokines and chemokines via the inhibition of IκB-α degradation and the resulting suppression of NF-κB activity.

Effect of HSP70 Expression on UVB-induced Epidermal DNA Damage—As described in the introduction, UVB irradiation damages DNA (formation of photo-products) directly (formation of products such as CPDs) and indirectly via the production of ROS (formation of products such as 8-OHdG). To examine the effect of HSP70 expression on UVB-induced DNA damage in the epidermis, we compared the time-course profile of the level of CPDs and 8-OHdG after irradiation with UVB between transgenic mice expressing HSP70 and wild-type mice. As shown in Fig. 6 (*A* and *B*), the level of 8-OHdG, judged from the intensity of immunohistochemical staining, was significantly lower in the epidermis of UVB-irradiated transgenic mice expressing HSP70 than in wild-type mice 1 h after the UVB irradiation (45 mJ/cm^2), suggesting that the UVB-induced formation of 8-OHdG is suppressed in the transgenic mice. Although the level of 8-OHdG 1 h after the irradiation was similar between wild-type mice irradiated with 45 mJ/cm^2 UVB and transgenic mice irradiated with 55 mJ/cm^2 UVB, the level was significantly lower in transgenic mice than in wild-type mice 48 h after the irradiation (Fig. 6, *A* and *B*), suggesting that the repair process of 8-OHdG is stimulated in transgenic mice expressing HSP70.

We also measured the level of CPDs in a similar manner. As shown in Fig. 6 (*C* and *D*), the number of CPD-positive cells was similar between wild-type mice and transgenic mice 1 h after the UVB irradiation. On the other hand, the number was significantly lower in transgenic mice than in wild-type mice 24 or 48 h after the UVB irradiation (Fig. 6, *C* and *D*). The results suggest that the repair rather than the formation of CPDs is affected by the expression of HSP70.

We then tested whether or not the effect of HSP70 expression on the formation and repair of 8-OHdG and CPDs can be reproduced *in vitro*. HSP70-overexpressing PAM212 cells and

mock transfectant control cells were irradiated with UVB, and the nuclear levels of 8-OHdG and CPDs were monitored by immunostaining. As shown in Fig. 7, *A* and *B*, HSP70-overexpressing cells showed a lower level of 8-OHdG than mock transfectant control cells 5 min after the UVB irradiation (50 mJ/cm^2), suggesting that the formation of 8-OHdG is suppressed by the expression of HSP70. Furthermore, comparing the level of 8-OHdG between HSP70-overexpressing cells irradiated with 65 mJ/cm^2 UVB and mock transfectant control cells irradiated with 50 mJ/cm^2 UVB, the initial (5 min after the UVB irradiation) levels were indistinguishable; however, the level was lower in HSP70-overexpressing cells than in mock transfectant control cells 24 h after the irradiation (Fig. 7, *A* and *B*), suggesting that the repair process of 8-OHdG is stimulated by the expression of HSP70. In other words, the protective effect of HSP70 against UVB-induced formation of 8-OHdG and its simulative effect on the repair process can be reproduced *in vitro*. On the other hand, the level of CPDs was indistinguishable between HSP70-overexpressing cells and mock transfectant control cells both 5 min and 24 h after the UVB irradiation, suggesting that neither the formation nor repair of CPDs is affected by the expression of HSP70. That is to say, the effect of HSP70 on the repair of CPDs was not reproduced *in vitro*.

The results in Fig. 6, *A* and *B*, suggest that UVB-induced ROS production in the skin is suppressed in transgenic mice expressing HSP70. On this basis, we measured the level of ROS in the skin by monitoring the lipid-derived free radical spin adduct with ESR spectroscopy and spin trap POBN, which reacts with ROS to form a radical spin adduct. As shown in Fig. 8*A*, a radical spin adduct of ESR spectrum similar to that reported in other organs was obtained (35–37, 44). The hyperfine coupling constants for the POBN radical adducts were $\alpha^N = 14.91 \pm 0.08$ G and $\alpha_b^H = 2.45 \pm 0.04$ G, which are similar to data previously reported for other organs (35–37, 44), suggesting that this ESR spectrum is derived from lipid-derived free radicals. As shown in Fig. 8*B*, the level of ROS in the skin was elevated by UVB irradiation in wild-type mice, and this increase was suppressed in transgenic mice expressing HSP70. This finding suggests that the expression of HSP70 suppresses UVB-induced ROS production in the skin.

TABLE 2
UVB-induced expression of pro-inflammatory cytokines and chemokines

Transgenic mice expressing HSP70 (HSP70 Tg) and wild-type mice (WT) were irradiated with or without 180 mJ/cm^2 UVB. In A, the dorsal skin was removed after 12 h (*mip-2*), 24 h (*il-6*, *mcp-1*), or 48 h (*il-1β*), and total RNA was extracted. Samples were subjected to real-time RT-PCR using a specific primer set for each gene. Values were normalized to the *gapdh* gene, expressed relative to the control sample. In B, the dorsal skin was removed after 48 h and skin homogenates were prepared. The amount of IL-1β and IL-6 was determined by using enzyme-linked immunosorbent assay. Values are mean ± S.E. ($n = 6$–9).

	UVB (mJ/cm^2)	WT	HSP70 Tg
A) Relative expression			
il-1β	0	1.0 ± 0.11	1.6 ± 0.31
	180	24.7 ± 9.19	3.4 ± 0.10[a]
il-6	0	1.0 ± 0.17	0.48 ± 0.072
	180	10.6 ± 1.66	5.6 ± 0.92[a]
mip-2	0	1.0 ± 0.89	1.8 ± 1.62
	180	16.7 ± 1.13	8.3 ± 0.55[b]
mcp-1	0	1.0 ± 0.46	1.5 ± 0.32
	180	36.7 ± 0.40	15.1 ± 6.00[a]
B) ng/g tissue			
IL-1β	0	0.48 ± 0.12	0.84 ± 0.14
	180	27.9 ± 2.71	8.7 ± 1.00[a]
IL-6	0	1.2 ± 0.37	0.87 ± 0.19
	180	67.4 ± 1.66	36.4 ± 5.93[a]

[a] $p < 0.01$.
[b] $p < 0.05$.

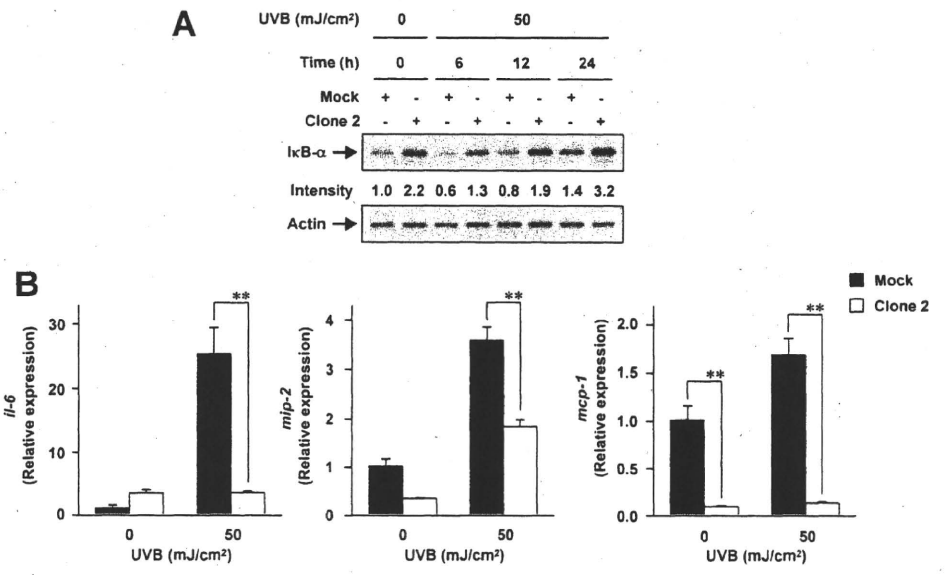

FIGURE 5. **Effect of HSP70 expression on UVB-induced decrease in the level of IκB-α and expression of pro-inflammatory cytokines and chemokines *in vitro*.** HSP70-overexpressing PAM212 cells (*Clone 2*) and mock transfectant control cells (*Mock*) were irradiated with or without 50 mJ/cm^2 UVB and incubated for indicated periods (*A*) or 6 h (*mip-2*), 12 h (*il-6*), or 24 h (*mcp-1*) (*B*). *A*, the expression of IκB-α was estimated by immunoblotting and shown as described in the legend of Fig. 3. *B*, mRNA expression of each gene was monitored as described in the legend of Table 2. Values are mean ± S.E. ($n = 3$). **, $p < 0.01$.

DISCUSSION

An ameliorative effect of HSP70 due to its cytoprotective, anti-inflammatory, and molecular chaperone (quality control of proteins) properties has been reported for various diseases. For example, we have shown using transgenic mice that HSP70 protects against irritant-produced lesions in the stomach and small intestine and inflammatory bowel disease-related experimental colitis (30, 38–40). The potential therapeutic applicability of HSP70 for use in other diseases, such as neurodegenerative diseases, ischemia-reperfusion damage, and diabetes has also been suggested (9, 45). Interestingly, GGA, a leading anti-ulcer drug on the Japanese market, has been reported to be an HSP inducer, up-regulating various HSPs not only in cultured gastric mucosal cells but also in various tissues *in vivo* (41). It was reported that GGA suppresses not only gastric lesions but also lesions of the small intestine, inflammatory bowel disease-related experimental colitis, and neurodegenerative diseases (39, 40, 46, 47). On the other hand, the use of HSP70 inducers in cosmetics

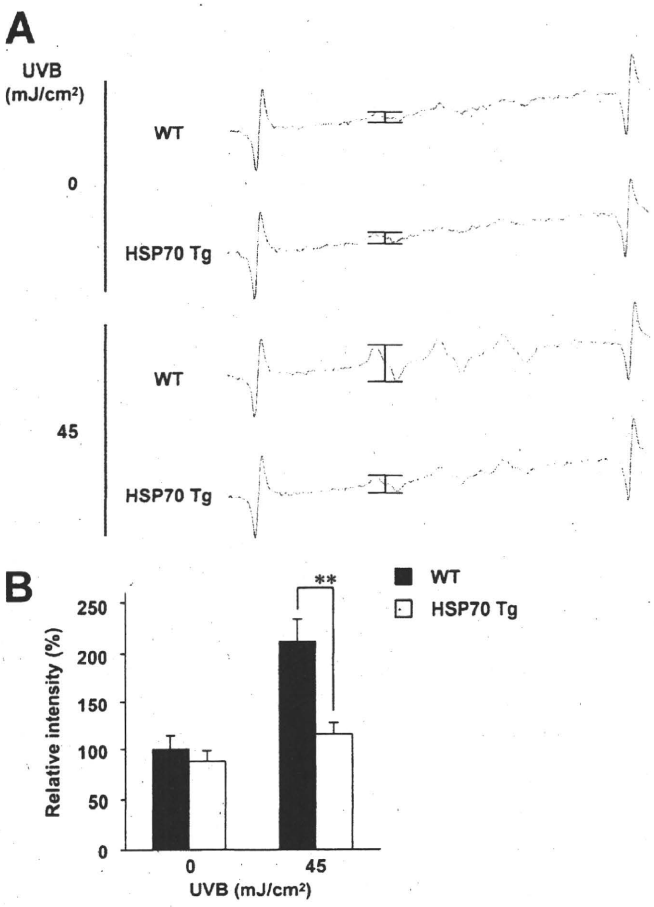

FIGURE 8. **UVB-induced increase in the epidermal ROS level.** Transgenic mice expressing HSP70 (*HSP70 Tg*) and wild-type mice (*WT*) were irradiated with 45 mJ/cm^2 UVB. *A*, POBN was administered, and the dorsal skin was removed after 1 h and subjected to radical adduct ESR spectrum analysis. *B*, the intensity of the ESR signal of the radical adduct (shown by the *bar* in *A*) was determined, expressed relative to the control sample, and given as the mean ± S.E. ($n = 6-10$). **, $p < 0.01$.

found that their HSP70-inducing activities were more potent than GGA.[4] We hope to develop some of these extracts as hypopigmenting (whitening) cosmetics or as drugs to combat melanin-related diseases.

Acknowledgments—We thank Drs. C. E. Angelidis and G. N. Pagoulatos (University of Ioannina, Greece) for generously providing transgenic mice expressing HSP70.

REFERENCES

1. Rabe, J. H., Mamelak, A. J., McElgunn, P. J., Morison, W. L., and Sauder, D. N. (2006) *J. Am. Acad. Dermatol.* **55,** 1–19
2. Svobodova, A., Walterova, D., and Vostalova, J. (2006) *Biomed. Pap. Med. Fac. Univ. Palacky. Olomouc. Czech. Repub.* **150,** 25–38
3. Matsumura, Y., and Ananthaswamy, H. M. (2004) *Toxicol. Appl. Pharmacol.* **195,** 298–308
4. Gröne, A. (2002) *Vet. Immunol. Immunopathol.* **88,** 1–12
5. Fisher, G. J., Wang, Z. Q., Datta, S. C., Varani, J., Kang, S., and Voorhees, J. J. (1997) *N. Engl. J. Med.* **337,** 1419–1428
6. Hoeijmakers, J. H. (2001) *Nature* **411,** 366–374
7. Budiyanto, A., Ahmed, N. U., Wu, A., Bito, T., Nikaido, O., Osawa, T., Ueda, M., and Ichihashi, M. (2000) *Carcinogenesis* **21,** 2085–2090
8. Simon, M. M., Reikerstorfer, A., Schwarz, A., Krone, C., Luger, T. A., Jäättelä, M., and Schwarz, T. (1995) *J. Clin. Invest.* **95,** 926–933
9. Morimoto, R. I., and Santoro, M. G. (1998) *Nat. Biotechnol.* **16,** 833–838
10. Wilson, N., McArdle, A., Guerin, D., Tasker, H., Wareing, P., Foster, C. S., Jackson, M. J., and Rhodes, L. E. (2000) *J. Cutan. Pathol.* **27,** 176–182
11. Morris, S. D. (2002) *Clin. Exp. Dermatol.* **27,** 220–224
12. Trautinger, F., Trautinger, I., Kindås-Mügge, I., Metze, D., and Luger, T. A. (1993) *J. Invest. Dermatol.* **101,** 334–338
13. Jonak, C., Klosner, G., and Trautinger, F. (2006) *Int. J. Cosmet. Sci.* **28,** 233–241
14. Zhou, X., Tron, V. A., Li, G., and Trotter, M. J. (1998) *J. Invest. Dermatol.* **111,** 194–198
15. Trautinger, F., Kokesch, C., Klosner, G., Knobler, R. M., and Kindås-Mügge, I. (1999) *Exp. Dermatol.* **8,** 187–192
16. Trautinger, F. (2001) *J. Photochem. Photobiol. B* **63,** 70–77
17. Brunet, S., and Giacomoni, P. U. (1989) *Mutat. Res.* **219,** 217–224
18. Trautinger, F., Kindås-Mügge, I., Barlan, B., Neuner, P., and Knobler, R. M. (1995) *J. Invest. Dermatol.* **105,** 160–162
19. Maytin, E. V., Wimberly, J. M., and Kane, K. S. (1994) *J. Invest. Dermatol.* **103,** 547–553
20. Kwon, S. B., Young, C., Kim, D. S., Choi, H. O., Kim, K. H., Chung, J. H., Eun, H. C., Park, K. C., Oh, C. K., and Seo, J. S. (2002) *J. Dermatol. Sci.* **28,** 144–151
21. Trautinger, F., Knobler, R. M., Hönigsmann, H., Mayr, W., and Kindås-Mügge, I. (1996) *J. Invest. Dermatol.* **107,** 442–443
22. Kane, K. S., and Maytin, E. V. (1995) *J. Invest. Dermatol.* **104,** 62–67
23. Krappmann, D., Wegener, E., Sunami, Y., Esen, M., Thiel, A., Mordmuller, B., and Scheidereit, C. (2004) *Mol. Cell. Biol.* **24,** 6488–6500
24. Tang, D., Kang, R., Xiao, W., Wang, H., Calderwood, S. K., and Xiao, X. (2007) *J. Immunol.* **179,** 1236–1244
25. Chen, H., Wu, Y., Zhang, Y., Jin, L., Luo, L., Xue, B., Lu, C., Zhang, X., and Yin, Z. (2006) *FEBS Lett.* **580,** 3145–3152
26. Weiss, Y. G., Bromberg, Z., Raj, N., Raphael, J., Goloubinoff, P., Ben-Neriah, Y., and Deutschman, C. S. (2007) *Crit. Care. Med.* **35,** 2128–2138
27. Bases, R. (2006) *Cell Stress Chaperones* **11,** 240–249
28. Kenny, M. K., Mendez, F., Sandigursky, M., Kureekattil, R. P., Goldman, J. D., Franklin, W. A., and Bases, R. (2001) *J. Biol. Chem.* **276,** 9532–9536
29. Mendez, F., Kozin, E., and Bases, R. (2003) *Cell Stress Chaperones* **8,** 153–161
30. Tanaka, K., Namba, T., Arai, Y., Fujimoto, M., Adachi, H., Sobue, G., Takeuchi, K., Nakai, A., and Mizushima, T. (2007) *J. Biol. Chem.* **282,** 23240–23252
31. Bradford, M. M. (1976) *Anal. Biochem.* **72,** 248–254
32. Hoshino, T., Tsutsumi, S., Tomisato, W., Hwang, H. J., Tsuchiya, T., and Mizushima, T. (2003) *J. Biol. Chem.* **278,** 12752–12758
33. Fujimoto, M., Takaki, E., Hayashi, T., Kitaura, Y., Tanaka, Y., Inouye, S., and Nakai, A. (2005) *J. Biol. Chem.* **280,** 34908–34916
34. Namba, T., Hoshino, T., Tanaka, K., Tsutsumi, S., Ishihara, T., Mima, S., Suzuki, K., Ogawa, S., and Mizushima, T. (2007) *Mol. Pharmacol.* **71,** 860–870
35. Ishihara, T., Tanaka, K., Tasaka, Y., Namba, T., Suzuki, J., Ishihara, T., Okamoto, S., Hibi, T., Takenaga, M., Igarashi, R., Sato, K., Mizushima, Y., and Mizushima, T. (2009) *J. Pharmacol. Exp. Ther.* **328,** 152–164
36. Sato, K., Kadiiska, M. B., Ghio, A. J., Corbett, J., Fann, Y. C., Holland, S. M., Thurman, R. G., and Mason, R. P. (2002) *FASEB J.* **16,** 1713–1720
37. Sato, K., Akaike, T., Kohno, M., Ando, M., and Maeda, H. (1992) *J. Biol. Chem.* **267,** 25371–25377
38. Tanaka, K., Tsutsumi, S., Arai, Y., Hoshino, T., Suzuki, K., Takaki, E., Ito, T., Takeuchi, K., Nakai, A., and Mizushima, T. (2007) *Mol. Pharmacol.* **71,** 985–993
39. Asano, T., Tanaka, K., Yamakawa, N., Adachi, H., Sobue, G., Goto, H., Takeuchi, K., and Mizushima, T. (2009) *J. Pharmacol. Exp. Ther.* **330,** 458–467
40. Suemasu, S., Tanaka, K., Namba, T., Ishihara, T., Katsu, T., Fujimoto, M., Adachi, H., Sobue, G., Takeuchi, K., Nakai, A., and Mizushima, T. (2009) *J. Biol. Chem.* **284,** 19705–19715

[4] Yamashita, Y., Hoshino, T., Matsuda, M., Kobayashi, C., Tominaga, A., Nakamura, Y., Nakashima, K., Yokomizo, K., Ikeda, T., Mineda, K., Maji, D., Niwano, Y., and Mizushima, T. (2010) *Exp. Dermatol.*, in press.

41. Hirakawa, T., Rokutan, K., Nikawa, T., and Kishi, K. (1996) *Gastroenterology* **111,** 345–357
42. Takashima, A., and Bergstresser, P. R. (1996) *Photochem. Photobiol.* **63,** 397–400
43. Feldmeyer, L., Keller, M., Niklaus, G., Hohl, D., Werner, S., and Beer, H. D. (2007) *Curr. Biol.* **17,** 1140–1145
44. Namba, T., Tanaka, K., Ito, Y., Ishihara, T., Hoshino, T., Gotoh, T., Endo, M., Sato, K., and Mizushima, T. (2009) *Am. J. Pathol.* **174,** 1786–1798
45. Jana, N. R., Tanaka, M., Wang, G., and Nukina, N. (2000) *Hum. Mol. Genet.* **9,** 2009–2018
46. Ohkawara, T., Nishihira, J., Takeda, H., Miyashita, K., Kato, K., Kato, M., Sugiyama, T., and Asaka, M. (2005) *Scand. J. Gastroenterol.* **40,** 1049–1057
47. Ohkawara, T., Nishihira, J., Takeda, H., Katsurada, T., Kato, K., Yoshiki, T., Sugiyama, T., and Asaka, M. (2006) *Int. J. Mol. Med.* **17,** 229–234
48. Bickers, D. R., and Athar, M. (2006) *J. Invest. Dermatol.* **126,** 2565–2575
49. Kulms, D., Zeise, E., Pöppelmann, B., and Schwarz, T. (2002) *Oncogene* **21,** 5844–5851
50. Zylicz, M., King, F. W., and Wawrzynow, A. (2001) *EMBO J.* **20,** 4634–4638
51. Raj, D., Brash, D. E., and Grossman, D. (2006) *J. Invest. Dermatol.* **126,** 243–257
52. Guo, S., Wharton, W., Moseley, P., and Shi, H. (2007) *Cell Stress Chaperones* **12,** 245–254
53. Jantschitsch, C., and Trautinger, F. (2003) *Photochem. Photobiol. Sci.* **2,** 899–903
54. Zou, Y., Crowley, D. J., and Van Houten, B. (1998) *J. Biol. Chem.* **273,** 12887–12892
55. Ando, H., Kondoh, H., Ichihashi, M., and Hearing, V. J. (2007) *J. Invest. Dermatol.* **127,** 751–761
56. Bustamante, J., Bredeston, L., Malanga, G., and Mordoh, J. (1993) *Pigment. Cell. Res.* **6,** 348–353
57. Tanaka, K., Hasegawa, J., Asamitsu, K., and Okamoto, T. (2005) *J. Pharmacol. Exp. Ther.* **315,** 624–630

Am J Physiol Lung Cell Mol Physiol 298: L348–L360, 2010.
First published December 24, 2009; doi:10.1152/ajplung.00289.2009.

Therapeutic effect of lecithinized superoxide dismutase on bleomycin-induced pulmonary fibrosis

Ken-Ichiro Tanaka,[1] Tomoaki Ishihara,[1] Arata Azuma,[2] Shoji Kudoh,[2] Masahito Ebina,[3] Toshihiro Nukiwa,[3] Yukihiko Sugiyama,[4] Yuichi Tasaka,[1] Takushi Namba,[1] Tsutomu Ishihara,[1] Keizo Sato,[1] Yutaka Mizushima,[5] and Tohru Mizushima[1]

[1]*Graduate School of Medical and Pharmaceutical Sciences, Kumamoto University, Kumamoto;* [2]*Department of Internal Medicine, Division of Respiratory, Infection, and Oncology, Nippon Medical School, Tokyo;* [3]*Department of Respiratory Medicine, Tohoku University Graduate School of Medicine, Sendai;* [4]*Department of Medicine, Jichi Medical University, Tochigi; and* [5]*DDS Institute, The Jikei University School of Medicine, Tokyo, Japan*

Submitted 20 August 2009; accepted in final form 21 December 2009

Tanaka K, Ishihara T, Azuma A, Kudoh S, Ebina M, Nukiwa T, Sugiyama Y, Tasaka Y, Namba T, Ishihara T, Sato K, Mizushima Y, Mizushima T. Therapeutic effect of lecithinized superoxide dismutase on bleomycin-induced pulmonary fibrosis. *Am J Physiol Lung Cell Mol Physiol* 298: L348–L360, 2010. First published December 24, 2009; doi:10.1152/ajplung.00289.2009.—Idiopathic pulmonary fibrosis (IPF) is thought to involve inflammatory infiltration of leukocytes, lung injury induced by reactive oxygen species (ROS), in particular superoxide anion, and fibrosis (collagen deposition). No treatment has been shown to improve definitively the prognosis for IPF patients. Superoxide dismutase (SOD) catalyzes the dismutation of superoxide anion to hydrogen peroxide, which is subsequently detoxified by catalase. Lecithinized SOD (PC-SOD) has overcome clinical limitations of SOD, including low tissue affinity and low stability in plasma. In this study, we examined the effect of PC-SOD on bleomycin-induced pulmonary fibrosis. Severity of the bleomycin-induced fibrosis in mice was assessed by various methods, including determination of hydroxyproline levels in lung tissue. Intravenous administration of PC-SOD suppressed the bleomycin-induced increase in the number of leukocytes in bronchoalveolar lavage fluid. Bleomycin-induced collagen deposition and increased hydroxyproline levels in the lung were also suppressed in animals treated with PC-SOD, suggesting that PC-SOD suppresses bleomycin-induced pulmonary fibrosis. The dose-response profile of PC-SOD was bell-shaped, but concurrent administration of catalase restored the ameliorative effect at high doses of PC-SOD. Intratracheal administration or inhalation of PC-SOD also attenuated the bleomycin-induced inflammatory response and fibrosis. The bell-shaped dose-response profile of PC-SOD was not observed for these routes of administration. We consider that, compared with intravenous administration, inhalation of PC-SOD may be a more therapeutically beneficial route of administration due to the higher safety and quality of life of the patient treated with this drug.

idiopathic pulmonary fibrosis; reactive oxygen species

IDIOPATHIC PULMONARY FIBROSIS (IPF) is a progressive and devastating chronic lung condition with poor prognosis; the mean length of survival from the time of diagnosis is 2.8–4.2 years. IPF progresses insidiously and slowly, and acute exacerbation of IPF is a highly lethal clinical event (1, 4, 21, 36). Current agents for the treatment of IPF, such as steroids and immunosuppressors, have not been found to improve the prognosis (1, 2, 26, 47), thus requiring the development of new types of drugs to treat IPF. To evaluate candidate drugs, the bleomycin-induced pulmonary fibrosis animal model provides a convenient option for the study (33).

Although the etiology of IPF is not yet fully understood, recent studies have suggested that it is triggered by lung injury and inflammation [infiltration of leukocytes (such as alveolar macrophages, lymphocytes, and neutrophils) and activation of cytokines]. Reactive oxygen species (ROS) that are released from the activated leukocytes cause further lung injury and inflammation. On the other hand, ROS and activated cytokines, especially TGF-β1, stimulate abnormal fibrosis (abnormal wound repair and remodeling) that is characterized by collagen deposition (22, 40). TGF-β1 seems to stimulate the production of interstitial collagen through both activation of fibroblasts and transformation of epithelial cells to fibroblasts (epithelial-mesenchymal transition; EMT) (3, 6, 48). This abnormal process of fibrosis is responsible for the pulmonary dysfunction associated with IPF. Supporting this idea, genetic inhibition of neutrophil elastase, of the TGF-β1-dependent signal transduction pathway, or of collagen synthesis was reported to suppress the progress of bleomycin-induced pulmonary fibrosis (5, 9, 14, 52). However, it is not clear whether pharmacological inhibition of these factors can improve the prognosis for IPF in humans.

A number of previous studies have suggested that the cellular redox state, determined by the balance between ROS (such as the superoxide anion) and antioxidant molecules [such as superoxide dismutase (SOD) and glutathione], plays an important role in the pathogenesis of IPF. Pulmonary inflammatory cells prepared from IPF patients generated higher levels of ROS than those from controls (25, 45). An increase in the level of ROS was reported in pulmonary tissues, blood, and bronchoalveolar lavage fluid (BALF) of IPF patients and bleomycin-administered animals (8, 18, 38, 41). Genetic modulation that increases or decreases the pulmonary level of ROS resulted in stimulation or suppression, respectively, of bleomycin-induced pulmonary fibrosis (11, 29). Thus, antioxidant molecules have attracted considerable attention as therapeutic candidates for the treatment of IPF. In fact, administration of *N*-acetylcysteine (NAC), which stimulates the synthesis of glutathione, exhibited therapeutic effects on IPF patients and bleomycin-induced pulmonary fibrosis in animals (10, 30, 31, 39).

SOD catalyzes the dismutation of superoxide anion to hydrogen peroxide, which is subsequently detoxified to oxygen and water by catalase or glutathione peroxidase (23). A decreased level of SOD was observed both in IPF patients and in

Address for reprint requests and other correspondence: T. Mizushima, Graduate School of Medical and Pharmaceutical Sciences, Kumamoto Univ., 5-1 Oe-honmachi, Kumamoto 862-0973, Japan (e-mail: mizu@gpo.kumamoto-u.ac.jp).

animals with bleomycin-induced pulmonary fibrosis (37, 53), thus suggesting that increasing SOD could be of therapeutic benefit in the treatment of IPF. However, the low affinity of SOD to the cell membrane where superoxide anion is produced, and its low stability in plasma, with a half-life of only a few minutes, were obstacles to the application of SOD in a clinical setting (13, 16, 17, 46). As a result of this, various SOD drug delivery systems have been devised to help overcome these limitations (16, 17, 20, 51).

Among these applications, lecithinized SOD (PC-SOD) has potentially beneficial effects for the treatment of IPF. PC-SOD is lecithinized human Cu/Zn-SOD in which four phosphatidylcholine (PC) derivative molecules are covalently bound to each SOD dimer (17). In vitro experiments with cultured cells have shown that this modification drastically improves the cell membrane affinity of SOD without decreasing its activity (16, 17), whereas in vivo experiments have demonstrated that it also greatly improves plasma stability (17). In a phase I clinical study, intravenously administered PC-SOD (40–160 mg) had a terminal half-life of more than 24 h, with good safety and tolerability (7, 42), and recently published results of a phase II clinical study have shown that intravenously administered PC-SOD (40 or 80 mg) significantly improved the symptoms of patients of ulcerative colitis (UC), which also involves ROS-induced tissue damage (43). Furthermore, intravenously administered PC-SOD ameliorated bleomycin-induced pulmonary fibrosis in mouse (44, 50), suggesting that PC-SOD could be effective in the treatment of IPF patients. However, a bell-shaped dose-response profile of PC-SOD has been reported for its ameliorative effect against bleomycin-induced pulmonary fibrosis (44, 50). Furthermore, when considering the quality of life (QOL) of patients, the present clinical protocol of PC-SOD administration (daily intravenous infusion for 4 wk) is expected to be improved. In this study, we provide evidence that the ineffectiveness of higher doses of PC-SOD is due to the accumulation of hydrogen peroxide. Furthermore, based on the results obtained here, we propose that administration of PC-SOD by inhalation is a clinically viable option to improve the QOL of IPF patients treated with this drug.

MATERIALS AND METHODS

Chemicals and animals. Paraformaldehyde, FBS, catalase from bovine liver (1,340 U/mg), an antibody against human Cu/Zn-SOD, 4-(dimethylamino)-benzaldehyde (DMBA), chloramine T, potassium dichromate, phosphotungstic acid, phosphomolybdic acid, Orange G, and acid fuchsin were obtained from Sigma (St. Louis, MO). Bleomycin was from Nippon Kayaku (Tokyo, Japan). Novo-heparin (5,000 units) for injection was from Mochida Pharmaceutical (Tokyo, Japan). Chloral hydrate was from Nacalai Tesque (Kyoto, Japan). Diff-Quik was from Sysmex (Kobe, Japan). Terminal deoxynucleotidyl transferase was obtained from Toyobo (Osaka, Japan). Biotin 14-ATP and Alexa Fluor 488 conjugated with streptavidin were purchased from Invitrogen (Carlsbad, CA). An ELISA kit for TGF-β1 was from R&D Systems (Minneapolis, MN). Mounting medium for immunohistochemical analysis (Vectashield) was from Vector Laboratories (Burlingame, CA). Cytospin 4 was purchased from Thermo Electron, whereas L-hydroxyproline, sodium acetate, TCA, azophloxin, and aniline blue were from Wako Pure Chemicals (Tokyo, Japan). Xylidine ponceau was from Waldeck (Muenster, Germany), and Mayer's hematoxylin, 1% eosin alcohol solution, mounting medium for histological examination (malinol), and Weigert's iron hematoxylin were from Muto Pure Chemicals (Tokyo, Japan). PC-SOD (3,000 U/mg) was from our laboratory stock (17). DAPI was from Dojindo (Kumamoto, Japan). Wild-type mice (6–8 wk old, ICR, male) were used. The experiments and procedures described here were carried out in accordance with the Guide for the Care and Use of Laboratory Animals as adopted and promulgated by the National Institutes of Health, and were approved by the Animal Care Committee of Kumamoto University.

Administration of bleomycin, PC-SOD, and catalase. ICR mice maintained under anesthesia with chloral hydrate (500 mg/kg) were given one intratracheal injection of bleomycin (5 mg/kg) in PBS (1 ml/kg) by use of micropipette (p200) to induce an inflammatory response and fibrosis. PC-SOD and catalase were dissolved in 5% xylitol and administered intravenously (tail vein) or intratracheally. For control mice, 5% xylitol solution was administered. The first administration of PC-SOD was performed just before the bleomycin administration.

For administration of PC-SOD by inhalation, five mice were placed in a chamber (volume, 45 l) and maintained under normoxic and normocapnic conditions. PC-SOD was dissolved in 10 ml of 5% xylitol, and an ultrasonic nebulizer (NE-U17 from Omron, Tokyo, Japan) that was connected to the chamber was used to nebulize the entire volume of the PC-SOD solution in 30 min. For control mice, 5% xylitol solution was subjected to nebulizer. Mice were kept in the chamber for a further 10 min after the 30 min of nebulizing.

Preparation of BALF and cell count. BALF was collected by cannulating the trachea and lavaging the lung with 1 ml of sterile PBS containing 50 U/ml heparin (two times). About 1.8 ml of BALF was routinely recovered from each animal. The total cell number was counted using a hemocytometer. Cells were stained with Diff-Quik reagents, and the ratios of alveolar macrophages, lymphocytes, and neutrophils to total cells were determined. More than 100 cells were counted for each sample.

Histological and immunohistochemical analyses and TUNEL assay. Lung tissue samples were fixed in 4% buffered paraformaldehyde and then embedded in paraffin before being cut into 4-μm-thick sections.

For histological examination, sections were stained first with Mayer's hematoxylin and then with 1% eosin alcohol solution. Samples were mounted with malinol and inspected with the aid of an Olympus BX51 microscope.

For staining of collagen (Masson's trichrome staining), sections were sequentially treated with *solution A* [5% (wt/vol) potassium dichromate and 5% (wt/vol) trichloroacetic acid], Weigert's iron hematoxylin, *solution B* [1.25% (wt/vol) phosphotungstic acid and 1.25% (wt/vol) phosphomolybdic acid], 0.75% (wt/vol) Orange G solution, *solution C* [0.12% (wt/vol) xylidine ponceau, 0.04% (wt/vol) acid fuchsin, and 0.02% (wt/vol) azophloxin], 2.5% (wt/vol) phosphotungstic acid, and finally aniline blue solution. Samples were mounted with malinol and inspected with the aid of an Olympus BX51 microscope.

For immunohistochemical analysis, sections were treated with 20 μg/ml protease K for antigen activation and incubated with 0.3% hydrogen peroxide in methanol for removal of endogenous peroxidase. Sections were blocked with 2.5% goat serum for 10 min, incubated for 12 h with an antibody against human Cu/Zn-SOD (1:200 dilution) in the presence of 2.5% BSA, and then incubated for 1 h with peroxidase-labeled polymer conjugated to goat anti-mouse immunoglobulins. Then, 3, 3′-diaminobenzidine was applied to the sections, and the sections were finally incubated with Mayer's hematoxylin. Samples were mounted with malinol and inspected using a fluorescence microscope (Olympus BX51).

For the TUNEL assay, sections were incubated first with proteinase K (20 μg/ml) for 15 min at 37°C, then with TdTase and biotin 14-ATP for 1 h at 37°C, and finally with Alexa Fluor 488 conjugated with streptavidin and DAPI (5 μg/ml) for 2 h. Samples were mounted with Vectashield and inspected with the aid of a fluorescence microscope (Olympus BX51).

Hydroxyproline determination. Hydroxyproline content was determined as described (49). Briefly, the right lung was removed and homogenized in 0.5 ml of 5% TCA. After centrifugation, pellets were hydrolyzed in 0.5 ml of 10 N HCl for 16 h at 110°C. Each sample was incubated for 20 min at room temperature after addition of 0.5 ml of 1.4% (wt/vol) chloramine T solution and then incubated at 65°C for 10 min after addition of 0.5 ml of Ehrlich's reagent [1 M DMBA, 70% (vol/vol) isopropanol and 30% (vol/vol) perchloric acid]. Absorbance was measured at 550 nm, and the amount of hydroxyproline was determined.

Determination of the amount of PC-SOD, TGF-β1, and hydrogen peroxide in vivo. Determination of the amount of PC-SOD in serum and tissue was carried out as previously described (17). After administration of PC-SOD, the blood was collected, and serum samples were obtained by centrifugation. Furthermore, lungs were dissected, cut into small pieces, homogenized, and centrifuged to obtain the supernatants. The amount of PC-SOD in samples was determined using a human Cu/Zn-SOD ELISA kit (Bender MedSystem, Burlingame, CA). The amount of TGF-β1 in the lung tissue was also measured by ELISA according to the manufacturer's protocol.

For determination of hydrogen peroxide levels, lungs were dissected, cut into small pieces, suspended in PBS, and incubated for 30 min at 4°C with rotation. After centrifugation, the supernatants were applied to the NWLSS NWK-HYP01 assay kit (Northwest Life Science Specialties, Vancouver, WA).

Real-time RT-PCR analysis. Real-time RT-PCR was performed as previously described (32) with some modifications. Total RNA was extracted from pulmonary tissues using an RNeasy kit according to the manufacturer's protocol. Samples (2.5 μg RNA) were reverse-transcribed using a first-strand cDNA synthesis kit. Synthesized cDNA was used in real-time RT-PCR (Chromo 4 Instrument; Bio-Rad Laboratories, Hercules, CA) experiments using iQ SYBR GREEN Supermix and analyzed with Opticon Monitor Software. Specificity was confirmed by electrophoretic analysis of the reaction products and by inclusion of template- or reverse transcriptase-free controls. To normalize the amount of total RNA present in each reaction, actin cDNA was used as an internal standard.

Primers were designed using the Primer3 website. The primers used were (name: forward primer, reverse primer): *collagen type I*

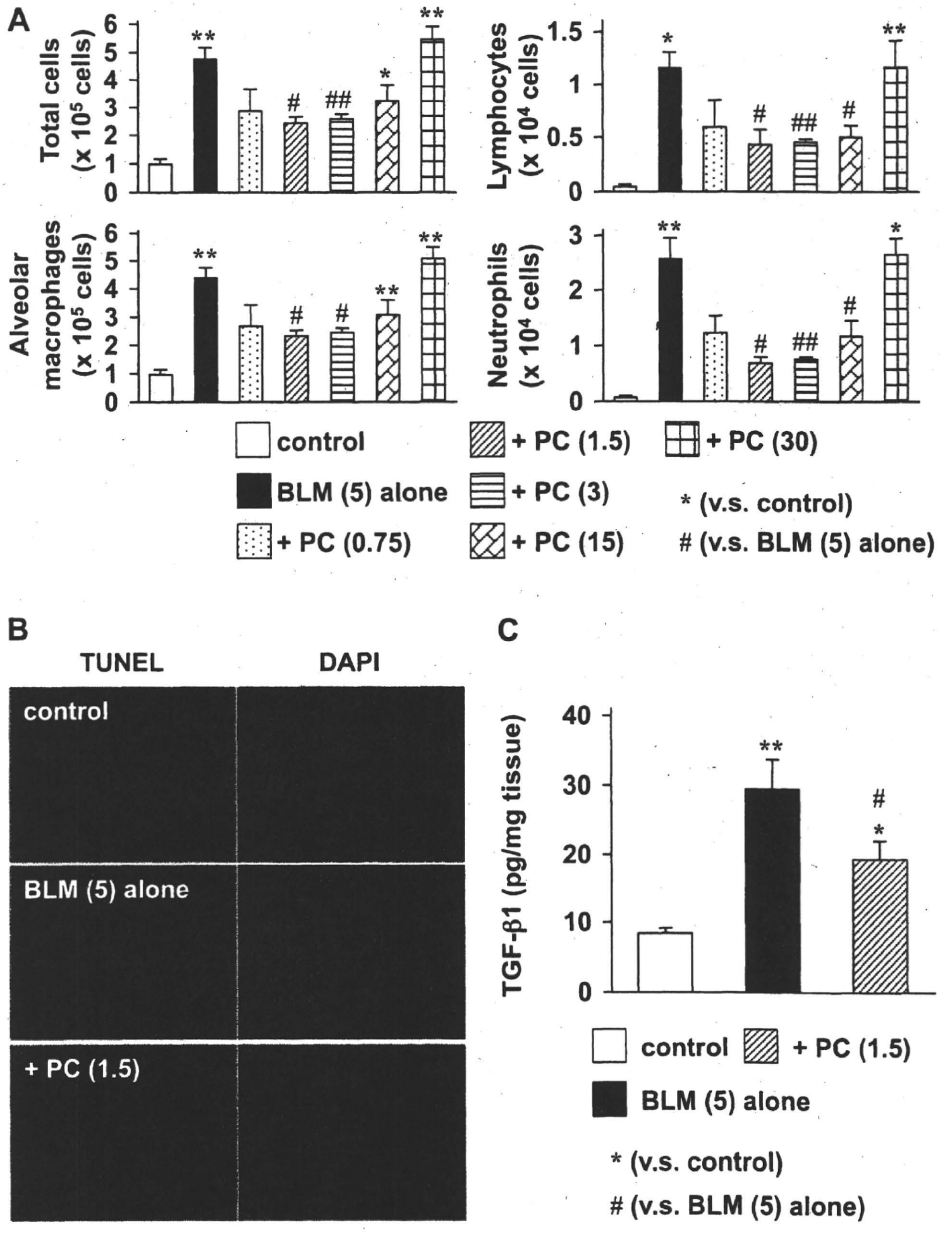

Fig. 1. Effect of intravenous administration of PC-SOD on bleomycin-induced inflammatory response. Mice treated with or without (vehicle) bleomycin (BLM) (5 mg/kg) once-only at *day 0* were intravenously administered indicated doses of PC-SOD (kU/kg) once per day for 3 days (*A–C*). Total cell number and numbers of alveolar macrophages, lymphocytes, and neutrophils were determined after 3 days as described in MATERIALS AND METHODS (*A*). Sections of pulmonary tissue were prepared after 3 days and subjected to TUNEL assay and DAPI staining. Similar results were obtained for at least 3 sections (*B*). The level of TGF-β1 in pulmonary tissue after 3 days was determined by ELISA (*C*). Values are means ± SE. * or #$P < 0.05$; ** or ##$P < 0.01$ (*A* and *C*).

(*Col1a1*): 5′-ccctgtctgcttcctgtaaact-3′, 5′-catgttcggttggtcaaagata-3′; *collagen type 3* (*Col1a3*): 5′-agggcagggaacaacttgatg-3′, 5′-ctccccttttgcacaaagctca-3′; *E-cadherin*: 5′-tgcccagaaaatgaaaaagg-3′, 5′-gtgtatgtggcaatgcgttc-3′; *Actin*: 5′-ggacttcgagcaagagatgg-3′, 5′- agcactgtgttggcgtacag-3′.

Statistical analysis. All values are expressed as means ± SE. Two-way ANOVA followed by the Tukey test or the Student's *t*-test for unpaired results was used to evaluate differences between more than three groups or between two groups, respectively. Differences were considered to be significant for values of $P < 0.05$.

RESULTS

Effect of PC-SOD on bleomycin-induced pulmonary fibrosis. Pulmonary fibrosis was induced in mice given a once-only (at *day 0*) intratracheal administration of bleomycin. The bleomycin-induced inflammatory response can be monitored as a function of the number of inflammatory cells (alveolar macrophages, lymphocytes, and neutrophils) in BALF 3 days after the administration of bleomycin. As shown in Fig. 1*A*, the total number of inflammatory cells and individual numbers of alveolar macrophages, lymphocytes, and neutrophils were all increased by the bleomycin treatment. This effect, however, could be suppressed by the simultaneous intravenous administration of PC-SOD, suggesting that PC-SOD ameliorates the bleomycin-induced pulmonary inflammatory response. PC-SOD produced a maximum beneficial effect at a dosage of 1.5–3 kU/kg, whereas a higher dose (30 kU/kg) did not suppress the bleomycin-induced pulmonary inflammatory response (bell-shaped dose-response profile) (Fig. 1*A*). Administration of the higher dose (30 kU/kg) of PC-SOD alone (without bleomycin administration) did not affect the number of inflammatory cells in BALF (data not shown).

Bleomycin-induced pulmonary fibrosis can be monitored by histopathological analysis and measurement of pulmonary hydroxyproline levels (an indicator of collagen levels) 14 days

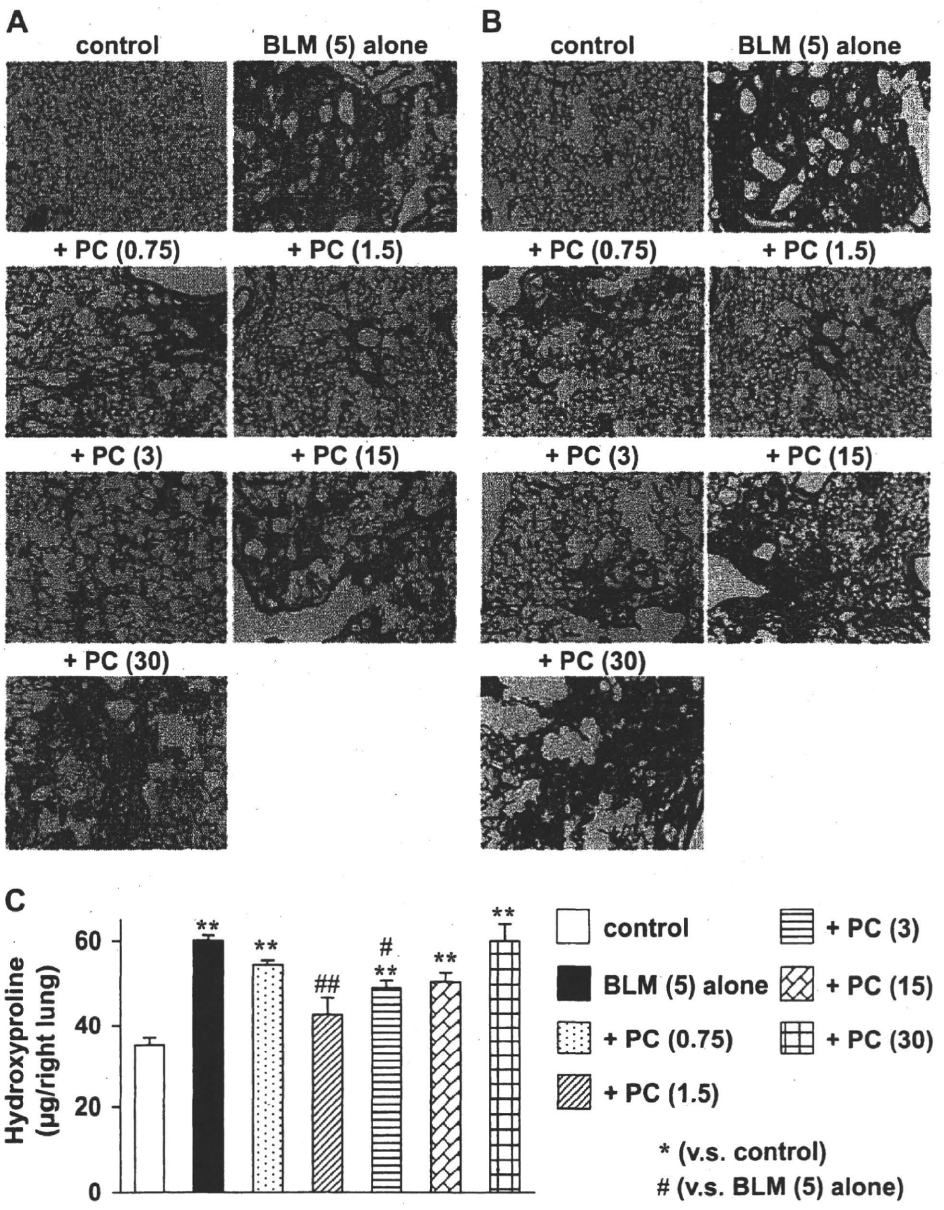

Fig. 2. Effect of intravenous administration of PC-SOD on bleomycin-induced pulmonary fibrosis. Mice treated once-only with or without (control) bleomycin (5 mg/kg) at *day 0* were intravenously administered indicated doses of PC-SOD (kU/kg) once per day for 14 days (*A–C*). Mice treated once-only with bleomycin (5 mg/kg) at *day 0* were intravenously administered indicated doses of PC-SOD (kU/kg) once per day from *day 7* to *day 13* (*D–F*). Sections of pulmonary tissue were prepared after 14 days and subjected to histopathological examination {H&E staining (*A* and *D*) or Masson's trichrome staining (*B* and *E*)] as described in MATERIALS AND METHODS. Similar results were obtained for at least 3 sections (*A*, *B*, *D*, *E*). The pulmonary hydroxyproline level was determined after 14 days as described in MATERIALS AND METHODS. Values are means ± SE. #$P <$ 0.05; ** or ##$P < 0.01$ (*C* and *F*).

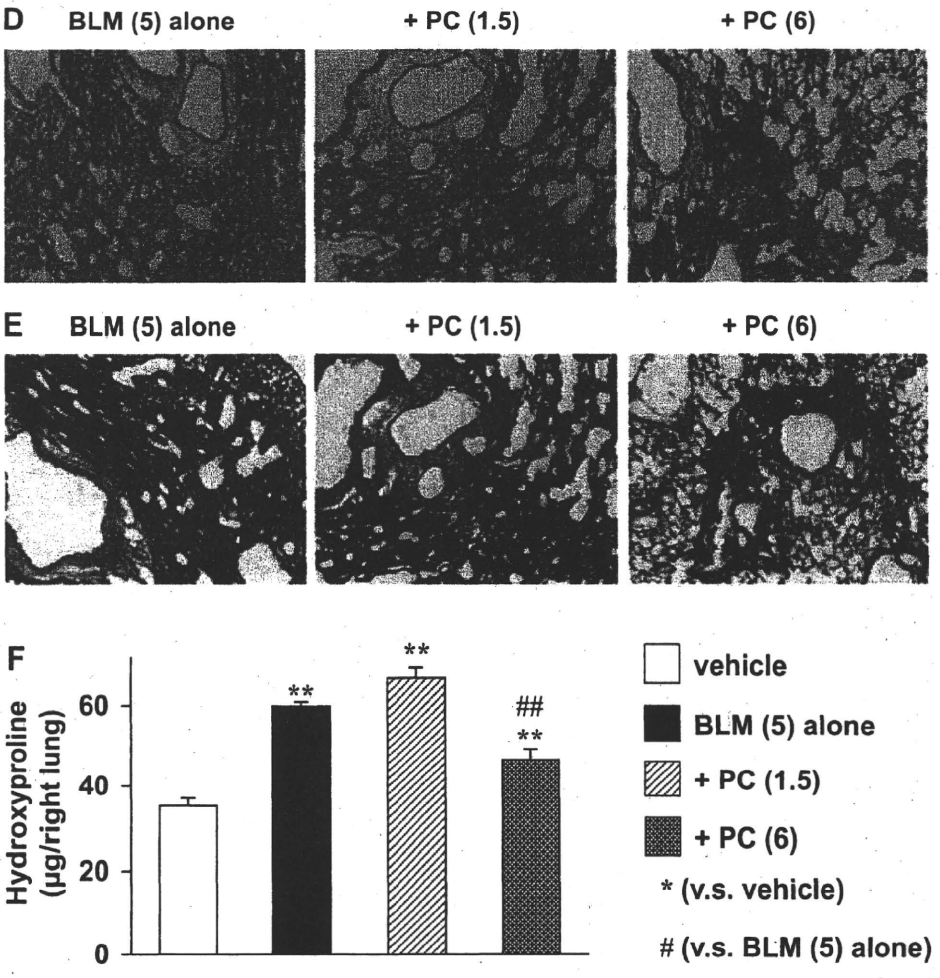

Fig. 2—*Continued*

after the administration of bleomycin. Histopathological analysis of pulmonary tissue using hematoxylin and eosin (H&E) staining revealed that the bleomycin administration induced severe pulmonary damage (thickened and edematous alveolar walls and interstitium) and infiltration of inflammatory cells into these regions (Fig. 2*A*). These phenomena were suppressed by the intravenous administration of PC-SOD (Fig. 2*A*). Again, a bell-shaped dose-response profile was observed; PC-SOD produced a maximum beneficial effect at 1.5–3 kU/kg, whereas at a higher dose (30 kU/kg) this ameliorative effect was not evident (Fig. 2*A*).

Masson's trichrome staining of collagen showed that bleomycin-induced collagen deposition was clearly suppressed by simultaneous intravenous administration of low doses (1.5–3.0 kU/kg) of PC-SOD, but not so clearly for a high dose (30 kU/kg) (Fig. 2*B*). As shown in Fig. 2*C*, a bell-shaped dose-response profile was also observed for the effect of PC-SOD on the bleomycin-induced elevation of pulmonary hydroxyproline content. The results in Fig. 2 thus support the fact that intravenous administration of PC-SOD ameliorates bleomycin-induced pulmonary fibrosis. We used an ELISA assay to determine the level of PC-SOD in serum and pulmonary tissue after its intravenous administration. As shown in Table 1, PC-SOD was detected in serum and pulmonary tissue 6 h after the final injection.

We also examined the effect of intravenous administration of PC-SOD on preexisting fibrosis; intravenous administration of PC-SOD was started at *day 7* after the administration of bleomycin. As shown in Fig. 2, *D–F*, bleomycin-induced

Table 1. *Serum and pulmonary levels of PC-SOD*

PC-SOD, Intravenous, kU/kg	*Plasma, U/ml*	*Lung, mU/mg Tissue*
0.75	7.80 ± 1.38	3.09 ± 0.84
1.5	16.9 ± 0.93	9.06 ± 1.29
15	128 ± 9.5	63.9 ± 1.86
30	245 ± 7.6	109 ± 4.3
PC-SOD, Intratracheal, kU/kg	*Plasma, U/ml*	*Lung, mU/mg Tissue*
0.15	n.d.	20.6 ± 10.5
0.75	0.30 ± 0.03	72.9 ± 5.31
1.5	0.75 ± 0.18	131 ± 28.6
15	5.34 ± 2.58	1,050 ± 381
30	12.5 ± 6.60	2,052 ± 702
60	26.6 ± 7.17	5,412 ± 183
PC-SOD, Inhalation, kU/Chamber	*Plasma, U/ml*	*Lung, mU/mg Tissue*
60	0.12 ± 0.06	22.7 ± 2.97
300	0.36 ± 0.12	51.9 ± 3.66
900	0.57 ± 0.12	198 ± 49.8

Mice treated with or without bleomycin (5 mg/kg) once-only at *day 0* were administered indicated doses of PC-SOD (kU/kg or kU/chamber) intravenously, intratracheally, or by inhalation once daily for 3 days. Blood and pulmonary tissue were taken 6 h after the final administration of PC-SOD. Levels of PC-SOD in samples were determined by ELISA. Values are means ± SE; n.d., not detected.

fibrosis was suppressed by a higher dose of PC-SOD (6 kU/kg) but not its low dose (1.5 kU/kg) under the conditions.

Mechanism for ameliorative effect of PC-SOD on bleomycin-induced pulmonary fibrosis. As described in the introduction, ROS-induced pulmonary cell death and TGF-β1-dependent stimulation of collagen synthesis and EMT play an important role in IPF and bleomycin-induced pulmonary fibrosis (24, 48). We examined effect of intravenous administration of PC-SOD on the extent of pulmonary cell death by employing the TUNEL assay. TUNEL-positive cells (indicative of cell death) increased in response to administration of bleomycin, and this increase was suppressed by simultaneous intravenous administration of PC-SOD (Fig. 1*B*), showing that PC-SOD protects pulmonary cells from cell death in vivo. We also examined the effect of PC-SOD on ROS-induced cell death in vitro, using A549 cells (human alveolar epithelial cell line). As shown in Fig. 3*A*, cell death induced by menadione, a superoxide anion-releasing drug, was inhibited by treatment of cells with PC-SOD.

A bleomycin-induced elevation of TGF-β1 levels in lung tissue was also suppressed by the intravenous administration of PC-SOD (Fig. 1*C*). We then examined effect of PC-SOD on the TGF-β1-dependent induction of collagen expression and EMT in vitro by using real-time RT-PCR analysis. Treatment of HFL-I cells (human embryonic lung fibroblast) with TGF-β1 induced the expression of *Col1a1* and *Col1a3* mRNA; the simultaneous treatment of cells with PC-SOD did not affect this induction (Fig. 3*B*). As shown in Fig. 3*C*, treatment of A549 cells with TGF-β1 induced or suppressed expression of *Col1a1* or *E-cadherin* mRNA, respectively, suggesting that

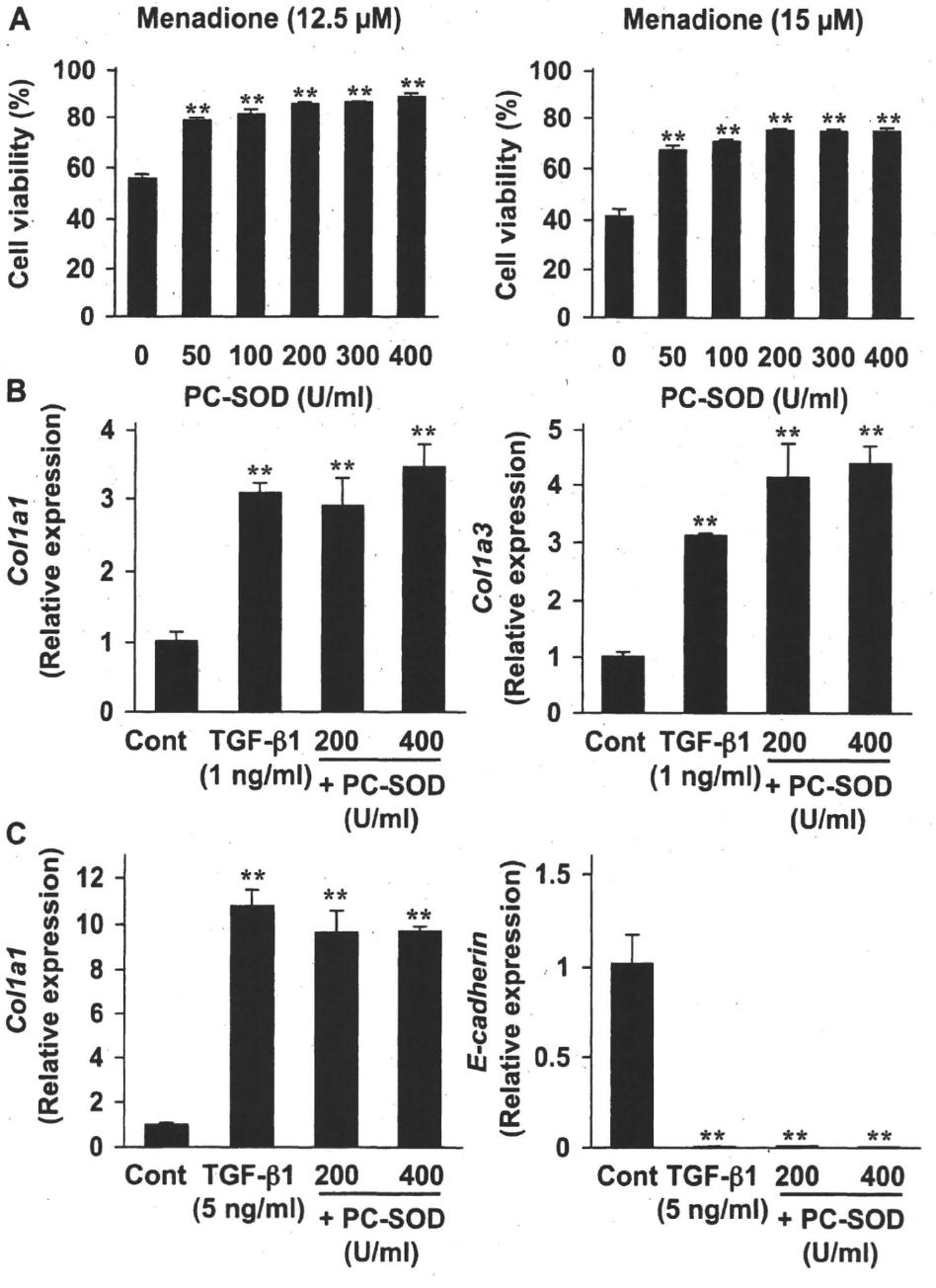

Fig. 3. Effect of PC-SOD on cell death and expression of collagen and epithelial-mesenchymal transition (EMT) in vitro. A549 (*A* and *C*) or HFL-I (*B*) cells were preincubated with the indicated concentration of PC-SOD for 1 h and further incubated with the indicated concentrations of menadione (*A*) or TGF-β1 (*B* and *C*) for 24 h in the presence of the same concentrations of PC-SOD as in the preincubation step. Cell viability was determined by MTT assay (*A*). Total RNA was extracted and subjected to real-time RT-PCR using a specific primer set for each gene. Values were normalized to the actin gene, expressed relative to the control sample (*B* and *C*). Values shown are means ± SE ($n = 3$). $^{**}P < 0.01$ (*A–C*).

EMT was induced. PC-SOD did not affect these TGF-β1-dependent alterations of mRNA expression (Fig. 3*C*). These results suggest that PC-SOD does not affect the TGF-β1-induced collagen synthesis and EMT.

Effect of simultaneous administration of catalase on the ameliorative effect of PC-SOD against bleomycin-induced pulmonary fibrosis. As described in the introduction, a bell-shaped dose-response profile of PC-SOD against bleomycin-induced pulmonary fibrosis has also been observed in other studies (44, 50). One possible explanation for the ineffectiveness of high doses of PC-SOD to combat the effects of bleomycin is the accumulation of hydrogen peroxide due to the relatively higher activity of SOD compared with catalase. We recently found evidence to support this notion in another animal model; simultaneous administration of catalase restored the ineffectiveness of higher doses of PC-SOD to combat dextran sulfate sodium-induced colitis, an animal model of UC (19). On this basis, we tested here the effect of concurrent administration of catalase on the activity of a high dose of PC-SOD in bleomycin-treated animals. Administration of 30 kU/kg PC-SOD improved the bleomycin-induced inflammatory response (increase in inflammatory cells in BALF) in the presence of the concurrent intravenous administration of catalase (1.5–6 kU/kg), but not in its absence (Fig. 4*A*). Administration of catalase alone did not significantly affect the bleomycin-induced inflammatory response (Fig. 4*A*).

We next examined the effect of simultaneous administration of catalase and high doses of PC-SOD on other aspects of bleomycin-induced pulmonary fibrosis. Bleomycin-induced pulmonary damage and infiltration of inflammatory cells into these regions were clearly suppressed by the simultaneous administration of catalase and a high dose of PC-SOD; however, treatment with either catalase or PC-SOD alone did not bring about such ameliorative effects (Fig. 4*B*). Collagen deposition and an increase in hydroxyproline levels were also clearly suppressed by the simultaneous

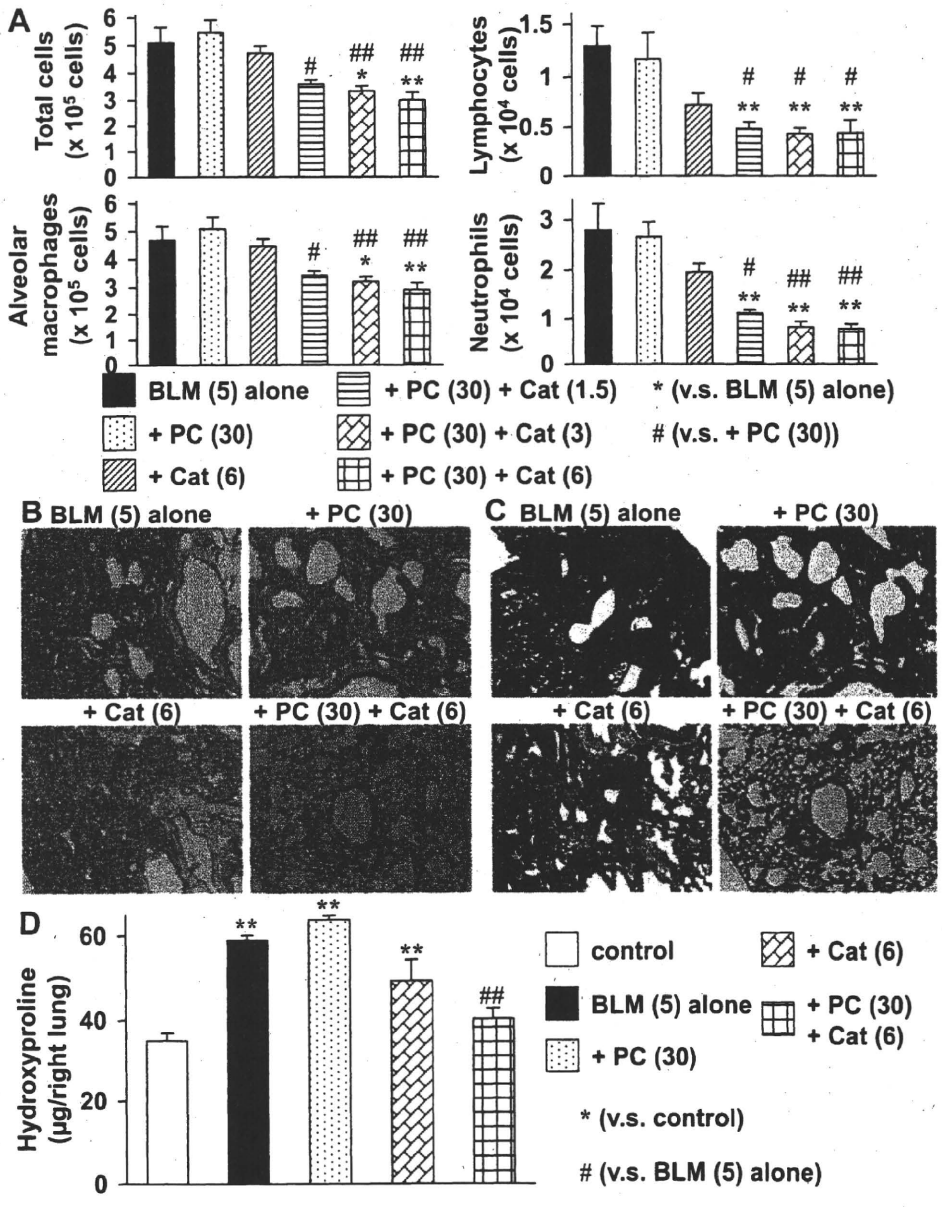

Fig. 4. Effect of concurrent administration of catalase on the ameliorative effect of PC-SOD on the bleomycin-induced inflammatory response and fibrosis. Mice were treated with bleomycin and PC-SOD, and the inflammatory response (*A*) and pulmonary fibrosis (*B–D*) were assessed as described in the legends of Figs. 1 and 2. The indicated dose of catalase (Cat) (kU/kg) was intravenously administered once per day for 3 days (*A*) or 14 days (*B–D*). Similar results were obtained for at least 3 sections (*B* and *C*). Values are means ± SE. * or #$P < 0.05$; ** or ##$P < 0.01$.

Table 2. *Effect of PC-SOD on pulmonary level of hydrogen peroxide*

PC-SOD, Intravenous, kU/kg	*Hydrogen Peroxide, μM*
Control	15.7 ± 0.81
1.5	17.4 ± 0.75
30	22.8 ± 1.33*
PC-SOD, Inhalation, kU/chamber	*Hydrogen Peroxide, μM*
Control	15.1 ± 1.79
60	13.1 ± 1.93
300	11.5 ± 0.95

Mice were administered indicated doses of PC-SOD (kU/kg or kU/chamber) intravenously or by inhalation once daily for 3 days. Lungs were removed, and the amount of hydrogen peroxide was determined. Values are means ± SE *$P < 0.01$; *vs. control.

administration of catalase and a high dose of PC-SOD (Fig. 4, *C* and *D*). Again, treatment with either catalase or a high dose of PC-SOD alone did not exert these beneficial effects (Fig. 4, *C* and *D*).

We further tested this idea by direct measurement of the pulmonary level of hydrogen peroxide. As shown in Table 2, administration of a high dose (30 kU/kg) but not a low dose (1.5 kU/kg) of PC-SOD increased the pulmonary level of hydrogen peroxide. The results shown in Fig. 4 and Table 2 suggest that the catalase-dependent restoration of efficacy of a high dose of PC-SOD on bleomycin-induced pulmonary fibrosis is due to the detoxification of hydrogen peroxide effects produced by a relatively higher activity of SOD.

Effect of modified methods of administration on PC-SOD's capacity to combat bleomycin-induced pulmonary fibrosis. To obtain some useful clues for refining the clinical guidelines for administration of PC-SOD, we tested the outcome of other routes of administration in the treatment of bleomycin-induced pulmonary fibrosis. As illustrated in Fig. 5*A*, the intratracheal administration of PC-SOD gave ameliorative effects against the bleomycin-induced inflammatory response. Interestingly, a bell-shaped dose-response profile was not observed with this

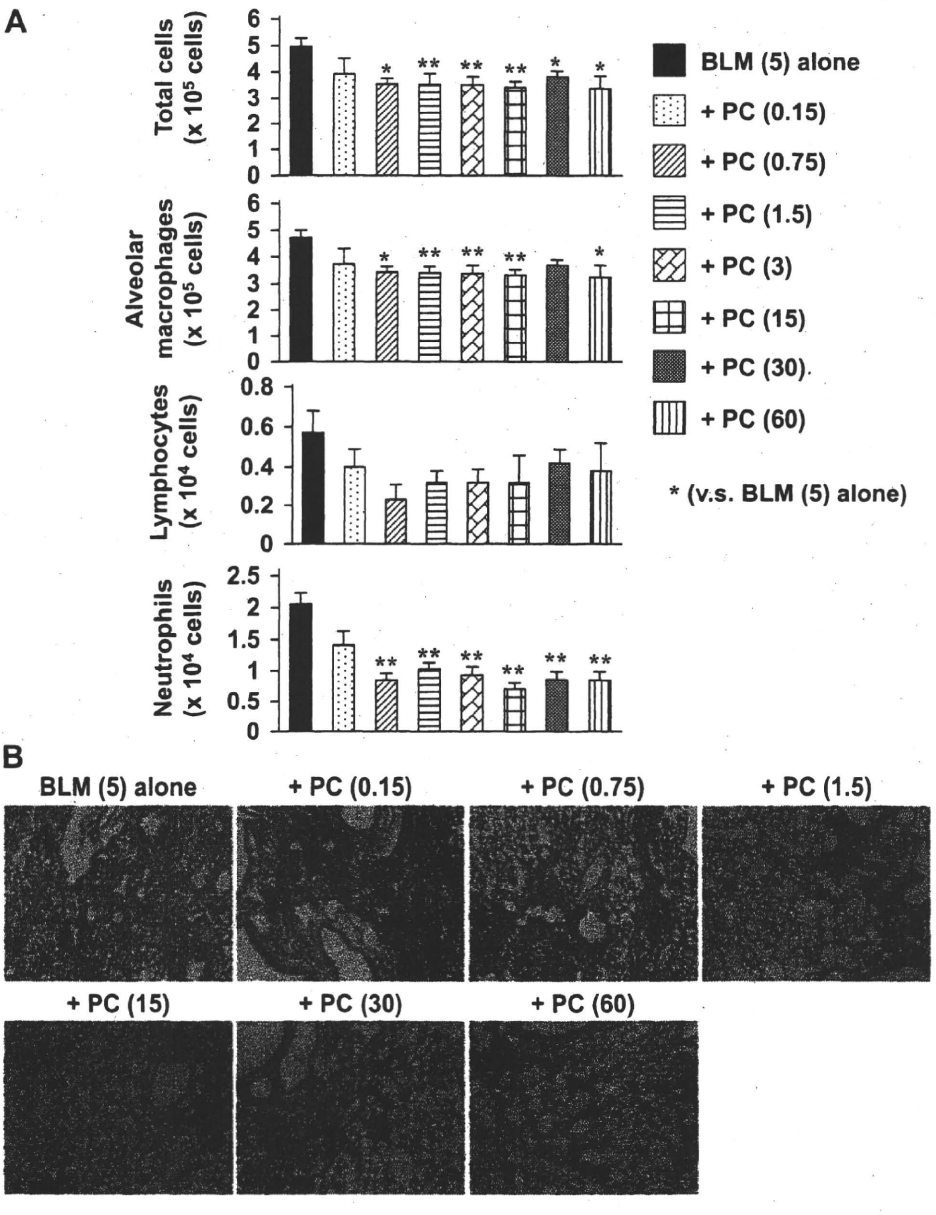

Fig. 5. Effect of intratracheal administration of PC-SOD on bleomycin-induced inflammatory response and pulmonary fibrosis. Mice were treated with bleomycin, and the inflammatory response (*A*) and pulmonary fibrosis (*B–D*) were assessed as described in the legends of Figs. 1 and 2. The indicated doses of PC-SOD (kU/kg) were administered intratracheally once per day for 3 days (*A*) or 14 days (*B–D*). Similar results were obtained for at least 3 sections (*B* and *C*). Values are means ± SE. * or #$P < 0.05$; ** or ##$P < 0.01$.

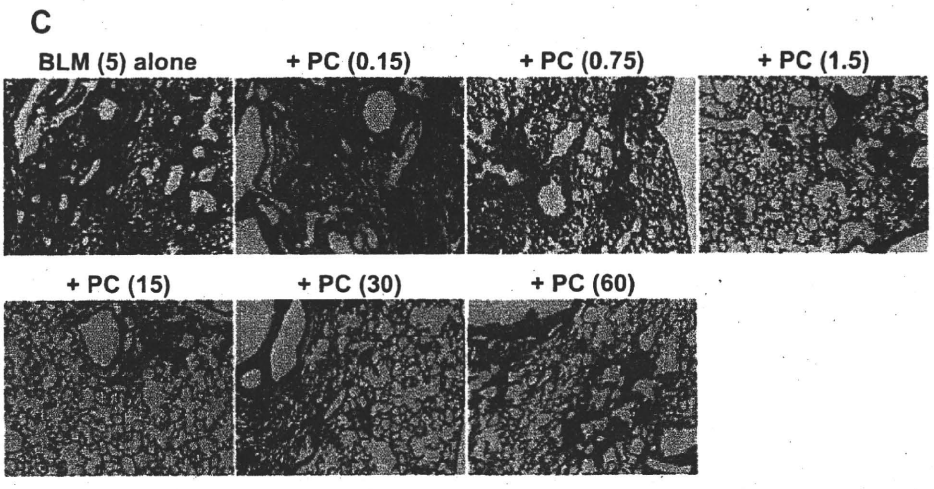

Fig. 5—*Continued*

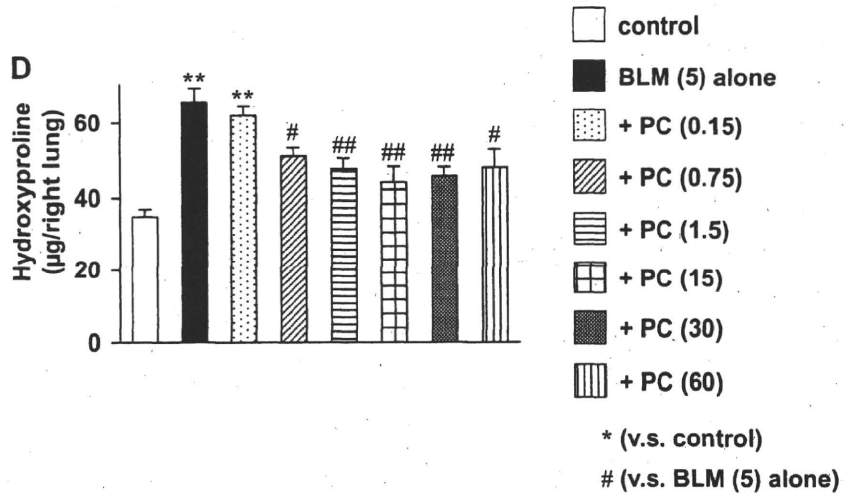

route of administration; the intratracheal administration of higher doses of PC-SOD (30 or 60 kU/kg) showed similar ameliorative effects to those seen for lower doses (Fig. 5*A*). As shown in Fig. 5, *B–D*, the intratracheal administration of PC-SOD also suppressed bleomycin-induced pulmonary tissue damage and fibrosis. Again, the bell-shape dose-response profile was not so obvious.

As shown in Table 1, after daily intratracheal administration of PC-SOD, the pulmonary level of PC-SOD was very high compared with that seen following intravenous administration. We therefore compared the distribution of PC-SOD in lung tissue in response to intravenous and intratracheal administration using immunohistochemical analysis with antibody against human Cu/Zn-SOD. As shown in Fig. 6, SOD was detected depending on the administration of PC-SOD, showing that this antibody specifically recognizes administered PC-SOD (not endogenous mouse SOD) under the conditions used. PC-SOD was detected in tissues containing a major airway but was not as evident in regions distant from trachea after the intratracheal administration of a low dose (1.5 kU/kg) (Fig. 6). On the other hand, PC-SOD was widely detected in both regions after the intravenous administration of a high dose (30 kU/kg) (Fig. 6). No SOD staining was observed in any regions after the intravenous administration of a low dose of PC-SOD (1.5 kU/kg) (data not shown).

PC-SOD was also detected in the serum after intratracheal administration; however, the level was much lower than that measured after its intravenous administration at an equivalent dose (Table 1).

The results shown in Fig. 5 suggest that inhalation of PC-SOD may increase the QOL of patients in the clinical practice. To test this idea, bleomycin-administered mice were placed in a chamber connected to an ultrasonic nebulizer, thus exposing them to PC-SOD-containing vapor. We confirmed by HPLC analysis and measurement of SOD activity that this treatment did not affect the structure and activity of the PC-SOD (data not shown). This treatment was repeated once daily for 3 days or 14 days, and bleomycin-induced pulmonary disorders were examined. As shown in Fig. 7*A*, inhaled PC-SOD [both low dose (60 kU/chamber) and high dose (300 kU/chamber)] ameliorated the bleomycin-induced inflammatory response and suppressed the pulmonary tissue damage and fibrosis (Fig. 7, *B–D*). We also found that inhalation of an even higher dose of PC-SOD (900 kU/chamber) decreased the bleomycin-induced inflammatory response as much as its low dose (60 kU/chamber) (data not shown), suggesting that bell-

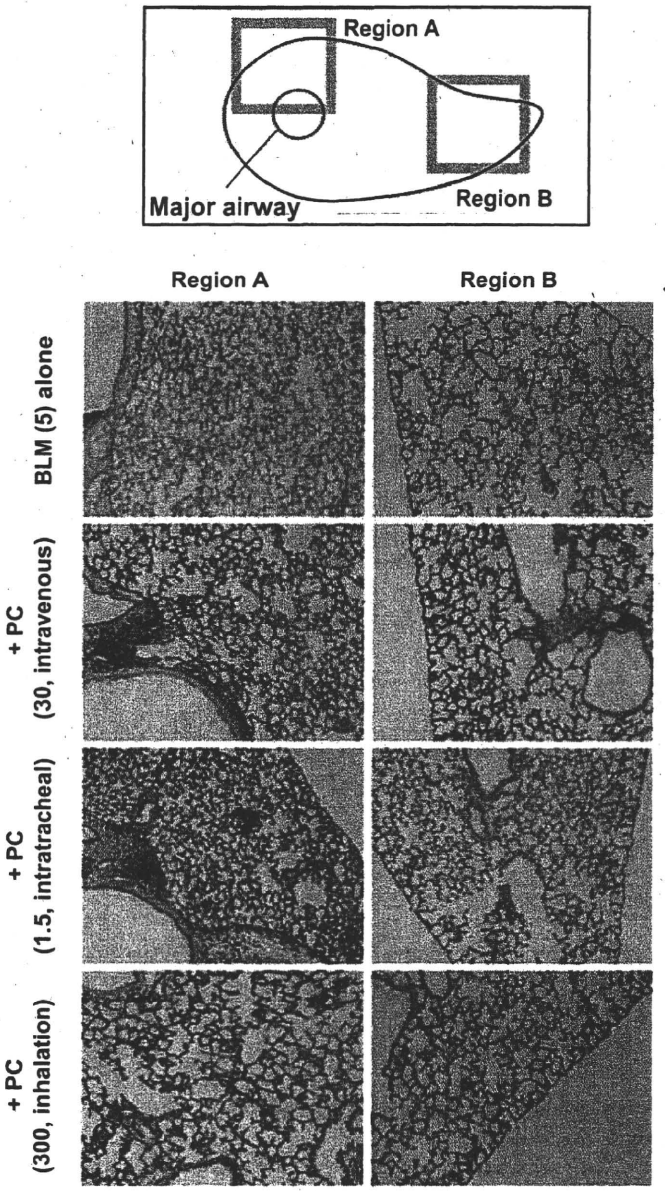

Fig. 6. Distribution of PC-SOD in the lung. Mice were treated with bleomycin, and indicated doses of PC-SOD (kU/kg or kU/chamber) were administered intravenously, intratracheally, or by inhalation once per day for 3 days. Sections of pulmonary tissue (from the 2 regions shown) were prepared 6 h after the final administration of PC-SOD (after 3 days) and subjected to immunohistochemical analysis with an antibody against human Cu/Zn-SOD. Similar results were obtained for at least 3 sections.

shaped dose-response profile did not occur with inhalation. As shown in Table 2, administration of not only a low dose (60 kU/chamber) but also a high dose (300 kU/chamber) of PC-SOD did not increase the pulmonary level of hydrogen peroxide, being different from the case of intravenous administration. We also found that inhalation of unmodified SOD did not affect the bleomycin-induced inflammatory response (Table 3). As shown in Table 1, PC-SOD was detected in the pulmonary tissue after daily sessions of inhalation. Immunohistochemical analysis revealed that inhaled PC-SOD was distributed broadly in the lung tissue (Fig. 6). Furthermore, very little PC-SOD was detected in serum following its delivery in this manner (Table 1).

DISCUSSION

Previous studies showed that intravenous administration of PC-SOD ameliorates bleomycin-induced pulmonary fibrosis; however, its molecular mechanism was not fully understood (44, 50). In these studies, a bell-shaped dose-response profile for PC-SOD was observed, but the mechanism underlying this effect was unclear. In the present study, we reproduced the results of the previous studies and examined underlying mechanisms. Furthermore, as the current clinical protocol for the administration of PC-SOD (once daily intravenous infusion for 4 wk) does not provide patients with good QOL, we attempted to find other dosing regimes in our animal model with a view to provide better clinical outcomes.

Pulmonary cell death could be a trigger of IPF and bleomycin-induced pulmonary fibrosis because it stimulates the inflammatory response and fibrosis (abnormal wound repair and remodeling) as described in the introduction. We showed that pulmonary cell death in bleomycin-treated mice was suppressed by administration of PC-SOD. We also showed that PC-SOD protected cultured lung epithelial cells from menadione-induced cell death. Furthermore, we found that PC-SOD suppresses the bleomycin-dependent increase in TGF-β1 levels in pulmonary tissue in vivo and menadione-induced production of TGF-β1 in vitro. On the other hand, PC-SOD did not affect the TGF-β1-dependent stimulation of collagen synthesis and induction of EMT. Based on these findings, we consider that PC-SOD ameliorates bleomycin-induced pulmonary fibrosis through its inhibitory effect on ROS-induced cell death and expression of TGF-β1 rather than by modulating TGF-β1-dependent cellular responses.

The bell-shaped dose-response profile of PC-SOD is of clinical concern, as this may reflect side effects of the drug. Here, however, we found that the efficacy of higher doses of PC-SOD is restored by simultaneous administration of catalase, which converts hydrogen peroxide to water and oxygen. As such, the ineffectiveness of high doses of PC-SOD on bleomycin-induced pulmonary fibrosis is likely to be caused by accumulation of hydrogen peroxide. The simultaneous administration of catalase with PC-SOD to IPF patients may therefore provide a greater therapeutic effect and lower the risk of side effects. Furthermore, the examination of catalase activity in individuals before PC-SOD administration may result in the establishment of safer treatment protocols for IPF patients.

We also found that intratracheal administration of PC-SOD significantly suppressed bleomycin-induced pulmonary fibrosis. PC-SOD was detected in the serum following this mode of administration; however, the serum level with intratracheal administration of PC-SOD (1.5 kU/kg, effective dose for bleomycin-induced pulmonary fibrosis) was much lower than that measured following the intravenous administration of PC-SOD (0.75 kU/kg, ineffective dose). Therefore, it seems that the delivery of PC-SOD directly to the lung (but not via the blood) is primarily responsible for the improved effects seen in response to its intratracheal administration. On the other hand, the pulmonary level of PC-SOD administered intravenously (1.5 kU/kg, effective dose) was much lower than that obtained with intratracheal administration (0.15 kU/kg, ineffective

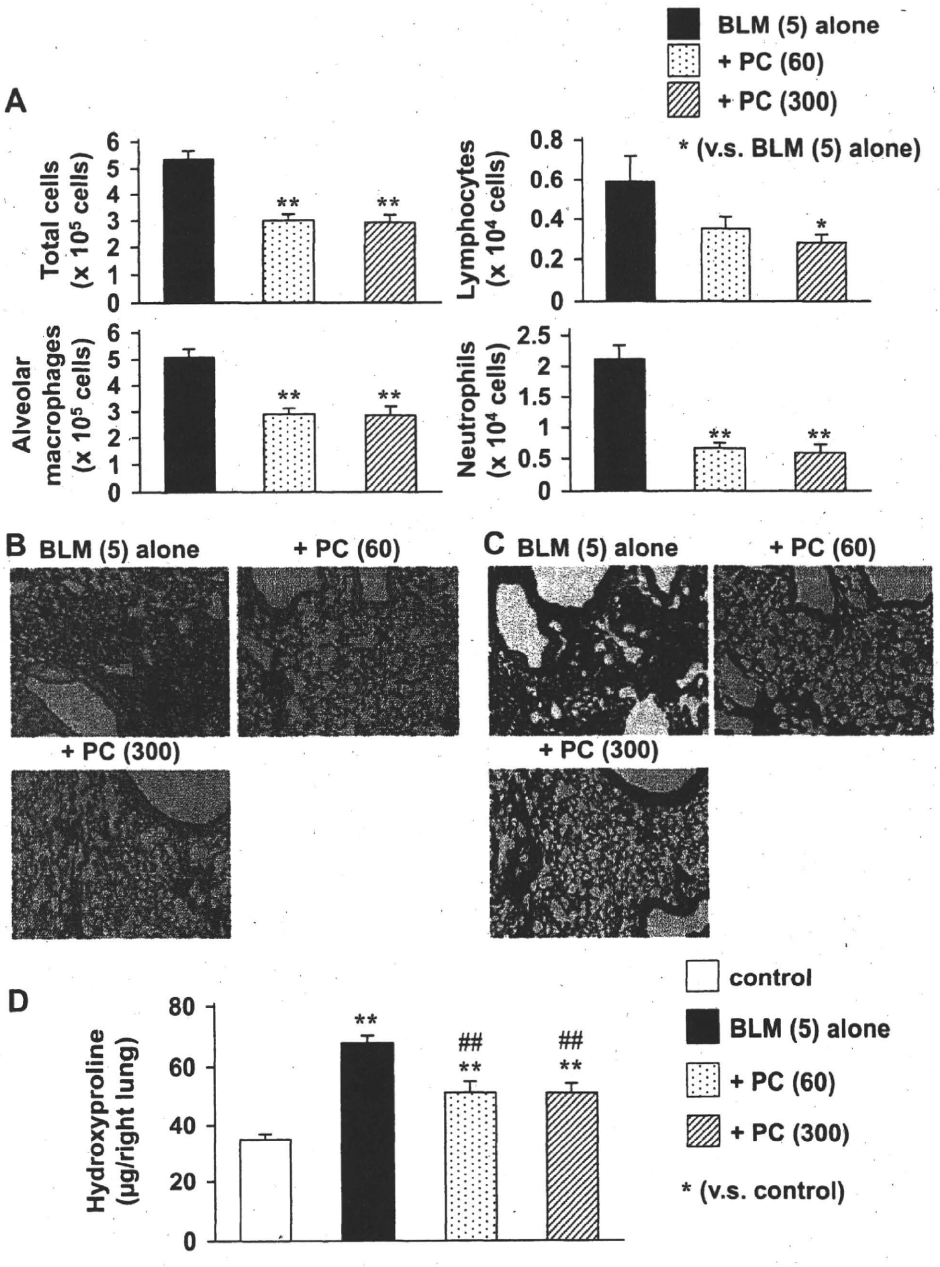

Fig. 7. Effect of inhalation of PC-SOD on bleomycin-induced inflammatory response and pulmonary fibrosis. Mice were treated with bleomycin, and the inflammatory response (*A*) and pulmonary fibrosis (*B–D*) were assessed as described in the legends of Figs. 1 and 2. The indicated doses of PC-SOD (kU/kg) were inhaled once per day for 3 days (*A*) or 14 days (*B–D*). Similar results were obtained for at least 3 sections (*B* and *C*). Values are means ± SE. $*P < 0.05$; ** or ##$P < 0.01$.

dose). This may due to the localization of intratracheally administered PC-SOD close to the trachea rather than regions distant from there. Therefore, it seems that PC-SOD should be delivered in a broad manner to the lung to suppress bleomycin-induced pulmonary fibrosis. It should also be noted that the bell-shaped dose-response profile of PC-SOD was not observed (up to 60 kU/kg) with the intratracheal mode of administration.

Table 3. *Effect of inhalation of U-SOD on bleomycin-induced inflammatory response*

U-SOD, Inhalation, kU/Chamber	Total Cells ($\times 10^5$ Cells)	Alveolar Macrophages ($\times 10^5$ Cells)	Lymphocytes ($\times 10^4$ Cells)	Neutrophils ($\times 10^4$ Cells)
Control	5.1 ± 0.28	4.8 ± 0.26	0.5 ± 0.01	1.7 ± 0.15
60	5.1 ± 0.14	4.8 ± 0.14	0.5 ± 0.07	1.6 ± 0.08
300	4.6 ± 0.23	4.4 ± 0.25	0.5 ± 0.08	1.5 ± 0.22

Mice were treated with bleomycin, and the inflammatory response was assessed as described in Fig. legend 1. Indicated doses of unmodified SOD (U-SOD; kU/chamber) were inhaled once per day for 3 days. Values are means ± SE.

We also found that inhalation of PC-SOD ameliorated bleomycin-induced pulmonary fibrosis. This finding is very important because if this mode of administration of PC-SOD can be applied clinically, it should greatly improve the QOL of patients treated with the drug. The lack of a bell-shaped dose-response profile with this route of administration is also therapeutically beneficial. The pulmonary level of PC-SOD after inhalation of PC-SOD (900 kU/chamber, effective dose) was higher than that after the intravenous administration (30 kU/kg, ineffective dose due to the bell-shaped profile). This discrepancy may be due to the difference in the local distribution of PC-SOD (for example, in the alveolar epithelia or in vessel

walls). It was recently reported that inhalation of NAC attenuates bleomycin-induced pulmonary fibrosis (15). Since NAC stimulates the conversion of hydrogen peroxide to water and oxygen (12, 27), simultaneous administration of PC-SOD and NAC by inhalation may have a synergistically therapeutic effect on bleomycin-induced pulmonary fibrosis and IPF.

A phase II clinical study has shown that intravenously administered PC-SOD (40 or 80 mg) showed therapeutic effects against IPF as judged by the serum level of markers (lactate dehydrogenase and surfactant protein A) (Azuma A, Ohta K, Sugiyama Y, Nukiwa T, Kudoh S, unpublished results). Based on results in this study, we propose that the inhalation mode for administering PC-SOD could prove beneficial for the treatment of IPF patients. This is because compared with intravenous administration, this mode of administration would cause improvement of the QOL of patients treated with the drug, equivalent efficacy (judged by immunohistochemical analysis in this study), and superior safety (due to lack of a bell-shaped dose-response profile). This mode of administration may be effective for other pulmonary diseases, such as chronic obstructive pulmonary disease and asthma, in which ROS-induced pulmonary damage also plays an important role (28, 34, 35).

GRANTS

This work was supported by Grants-in-Aid for Scientific Research from the Ministry of Health, Labor, and Welfare of Japan, as well as the Japan Science and Technology Agency, and Grants-in-Aid for Scientific Research from the Ministry of Education, Culture, Sports, Science, and Technology, Japan.

DISCLOSURES

No conflicts of interest are declared by the author(s).

REFERENCES

1. **American Thoracic Society.** Idiopathic pulmonary fibrosis: diagnosis and treatment. International consensus statement. American Thoracic Society and the European Respiratory Society. *Am J Respir Crit Care Med* 161: 646–664, 2000.
2. American Thoracic Society/European Respiratory Society. International Multidisciplinary Consensus Classification of the Idiopathic Interstitial Pneumonias. This joint statement of the American Thoracic Society and the European Respiratory Society was adopted by the ATS board of directors June 2001 and by the ERS Executive Committee June 2001. *Am J Respir Crit Care Med* 165: 277–304, 2002.
3. **Bartram U, Speer CP.** The role of transforming growth factor beta in lung development and disease. *Chest* 125: 754–765, 2004.
4. **Bjoraker JA, Ryu JH, Edwin MK, Myers JL, Tazelaar HD, Schroeder DR, Offord KP.** Prognostic significance of histopathologic subsets in idiopathic pulmonary fibrosis. *Am J Respir Crit Care Med* 157: 199–203, 1998.
5. **Bonniaud P, Margetts PJ, Ask K, Flanders K, Gauldie J, Kolb M.** TGF-beta and Smad3 signaling link inflammation to chronic fibrogenesis. *J Immunol* 175: 5390–5395, 2005.
6. **Border WA, Noble NA.** Transforming growth factor beta in tissue fibrosis. *N Engl J Med* 331: 1286–1292, 1994.
7. **Broeyer FJ, van Aken BE, Suzuki J, Kemme MJ, Schoemaker HC, Cohen AF, Mizushima Y, Burggraaf J.** The pharmacokinetics and effects of a long-acting preparation of superoxide dismutase (PC-SOD) in man. *Br J Clin Pharmacol* 65: 22–29, 2008.
8. **Cantin AM, North SL, Fells GA, Hubbard RC, Crystal RG.** Oxidant-mediated epithelial cell injury in idiopathic pulmonary fibrosis. *J Clin Invest* 79: 1665–1673, 1987.
9. **Chua F, Dunsmore SE, Clingen PH, Mutsaers SE, Shapiro SD, Segal AW, Roes J, Laurent GJ.** Mice lacking neutrophil elastase are resistant to bleomycin-induced pulmonary fibrosis. *Am J Pathol* 170: 65–74, 2007.
10. **Demedts M, Behr J, Buhl R, Costabel U, Dekhuijzen R, Jansen HM, MacNee W, Thomeer M, Wallaert B, Laurent F, Nicholson AG, Verbeken EK, Verschakelen J, Flower CD, Capron F, Petruzzelli S, De Vuyst P, van den Bosch JM, Rodriguez-Becerra E, Corvasce G, Lankhorst I, Sardina M, Montanari M.** High-dose acetylcysteine in idiopathic pulmonary fibrosis. *N Engl J Med* 353: 2229–2242, 2005.
11. **Fattman CL, Chang LY, Termin TA, Petersen L, Enghild JJ, Oury TD.** Enhanced bleomycin-induced pulmonary damage in mice lacking extracellular superoxide dismutase. *Free Radic Biol Med* 35: 763–771, 2003.
12. **Gillissen A, Nowak D.** Characterization of *N*-acetylcysteine and ambroxol in anti-oxidant therapy. *Respir Med* 92: 609–623, 1998.
13. **Greenwald RA.** Superoxide dismutase and catalase as therapeutic agents for human diseases. A critical review. *Free Radic Biol Med* 8: 201–209, 1990.
14. **Hagiwara S, Iwasaka H, Matsumoto S, Noguchi T.** Antisense oligonucleotide inhibition of heat shock protein (HSP) 47 improves bleomycin-induced pulmonary fibrosis in rats. *Respir Res* 8: 37, 2007.
15. **Hagiwara SI, Ishii Y, Kitamura S.** Aerosolized administration of *N*-acetylcysteine attenuates lung fibrosis induced by bleomycin in mice. *Am J Respir Crit Care Med* 162: 225–231, 2000.
16. **Igarashi R, Hoshino J, Ochiai A, Morizawa Y, Mizushima Y.** Lecithinized superoxide dismutase enhances its pharmacologic potency by increasing its cell membrane affinity. *J Pharmacol Exp Ther* 271: 1672–1677, 1994.
17. **Igarashi R, Hoshino J, Takenaga M, Kawai S, Morizawa Y, Yasuda A, Otani M, Mizushima Y.** Lecithinization of superoxide dismutase potentiates its protective effect against Forssman antiserum-induced elevation in guinea pig airway resistance. *J Pharmacol Exp Ther* 262: 1214–1219, 1992.
18. **Inghilleri S, Morbini P, Oggionni T, Barni S, Fenoglio C.** In situ assessment of oxidant and nitrogenic stress in bleomycin pulmonary fibrosis. *Histochem Cell Biol* 125: 661–669, 2006.
19. **Ishihara T, Tanaka K, Tasaka Y, Namba T, Suzuki J, Okamoto S, Hibi T, Takenaga M, Igarashi R, Sato K, Mizushima Y, Mizushima T.** Therapeutic effect of lecithinized superoxide dismutase against colitis. *J Pharmacol Exp Ther* 328: 152–164, 2009.
20. **Keshavarzian A, Morgan G, Sedghi S, Gordon JH, Doria M.** Role of reactive oxygen metabolites in experimental colitis. *Gut* 31: 786–790, 1990.
21. **Kim DS, Collard HR, King TE Jr.** Classification and natural history of the idiopathic interstitial pneumonias. *Proc Am Thorac Soc* 3: 285–292, 2006.
22. **Kinnula VL, Myllarniemi M.** Oxidant-antioxidant imbalance as a potential contributor to the progression of human pulmonary fibrosis. *Antioxid Redox Signal* 10: 727–738, 2008.
23. **Kruidenier L, Verspaget HW.** Review article: oxidative stress as a pathogenic factor in inflammatory bowel disease–radicals or ridiculous? *Aliment Pharmacol Ther* 16: 1997–2015, 2002.
24. **Kuwano K, Hagimoto N, Maeyama T, Fujita M, Yoshimi M, Inoshima I, Nakashima N, Hamada N, Watanabe K, Hara N.** Mitochondria-mediated apoptosis of lung epithelial cells in idiopathic interstitial pneumonias. *Lab Invest* 82: 1695–1706, 2002.
25. **Kuwano K, Nakashima N, Inoshima I, Hagimoto N, Fujita M, Yoshimi M, Maeyama T, Hamada N, Watanabe K, Hara N.** Oxidative stress in lung epithelial cells from patients with idiopathic interstitial pneumonias. *Eur Respir J* 21: 232–240, 2003.
26. **Luppi F, Cerri S, Beghe B, Fabbri LM, Richeldi L.** Corticosteroid and immunomodulatory agents in idiopathic pulmonary fibrosis. *Respir Med* 98: 1035–1044, 2004.
27. **MacNee W, Rahman I.** Is oxidative stress central to the pathogenesis of chronic obstructive pulmonary disease? *Trends Mol Med* 7: 55–62, 2001.
28. **Macnee W, Rahman I.** Oxidants and antioxidants as therapeutic targets in chronic obstructive pulmonary disease. *Am J Respir Crit Care Med* 160: S58–S65, 1999.
29. **Manoury B, Nenan S, Leclerc O, Guenon I, Boichot E, Planquois JM, Bertrand CP, Lagente V.** The absence of reactive oxygen species production protects mice against bleomycin-induced pulmonary fibrosis. *Respir Res* 6: 11, 2005.
30. **Meyer A, Buhl R, Kampf S, Magnussen H.** Intravenous *N*-acetylcysteine and lung glutathione of patients with pulmonary fibrosis and normals. *Am J Respir Crit Care Med* 152: 1055–1060, 1995.
31. **Meyer A, Buhl R, Magnussen H.** The effect of oral *N*-acetylcysteine on lung glutathione levels in idiopathic pulmonary fibrosis. *Eur Respir J* 7: 431–436, 1994.

32. **Mima S, Tsutsumi S, Ushijima H, Takeda M, Fukuda I, Yokomizo K, Suzuki K, Sano K, Nakanishi T, Tomisato W, Tsuchiya T, Mizushima T.** Induction of claudin-4 by nonsteroidal anti-inflammatory drugs and its contribution to their chemopreventive effect. *Cancer Res* 65: 1868–1876, 2005.
33. **Moore BB, Hogaboam CM.** Murine models of pulmonary fibrosis. *Am J Physiol Lung Cell Mol Physiol* 294: L152–L160, 2008.
34. **Nadeem A, Chhabra SK, Masood A, Raj HG.** Increased oxidative stress and altered levels of antioxidants in asthma. *J Allergy Clin Immunol* 111: 72–78, 2003.
35. **Nadeem A, Raj HG, Chhabra SK.** Increased oxidative stress and altered levels of antioxidants in chronic obstructive pulmonary disease. *Inflammation* 29: 23–32, 2005.
36. **Nagai S, Kitaichi M, Hamada K, Nagao T, Hoshino Y, Miki H, Izumi T.** Hospital-based historical cohort study of 234 histologically proven Japanese patients with IPF. *Sarcoidosis Vasc Diffuse Lung Dis* 16: 209–214, 1999.
37. **Nakatani-Okuda A, Ueda H, Kashiwamura S, Sekiyama A, Kubota A, Fujita Y, Adachi S, Tsuji Y, Tanizawa T, Okamura H.** Protection against bleomycin-induced lung injury by IL-18 in mice. *Am J Physiol Lung Cell Mol Physiol* 289: L280–L287, 2005.
38. **Scheule RK, Perkins RC, Hamilton R, Holian A.** Bleomycin stimulation of cytokine secretion by the human alveolar macrophage. *Am J Physiol Lung Cell Mol Physiol* 262: L386–L391, 1992.
39. **Serrano-Mollar A, Closa D, Prats N, Blesa S, Martinez-Losa M, Cortijo J, Estrela JM, Morcillo EJ, Bulbena O.** In vivo antioxidant treatment protects against bleomycin-induced lung damage in rats. *Br J Pharmacol* 138: 1037–1048, 2003.
40. **Sheppard D.** Transforming growth factor beta: a central modulator of pulmonary and airway inflammation and fibrosis. *Proc Am Thorac Soc* 3: 413–417, 2006.
41. **Strausz J, Muller-Quernheim J, Steppling H, Ferlinz R.** Oxygen radical production by alveolar inflammatory cells in idiopathic pulmonary fibrosis. *Am Rev Respir Dis* 141: 124–128, 1990.
42. **Suzuki J, Broeyer F, Cohen A, Takebe M, Burggraaf J, Mizushima Y.** Pharmacokinetics of PC-SOD, a lecithinized recombinant superoxide dismutase, after single- and multiple-dose administration to healthy Japanese and Caucasian volunteers. *J Clin Pharmacol* 48: 184–192, 2008.
43. **Suzuki Y, Matsumoto T, Okamoto S, Hibi T.** A lecithinized superoxide dismutase (PC-SOD) improves ulcerative colitis. *Colorectal Dis* 10: 931–934, 2008.
44. **Tamagawa K, Taooka Y, Maeda A, Hiyama K, Ishioka S, Yamakido M.** Inhibitory effects of a lecithinized superoxide dismutase on bleomycin-induced pulmonary fibrosis in mice. *Am J Respir Crit Care Med* 161: 1279–1284, 2000.
45. **Teramoto S, Fukuchi Y, Uejima Y, Shu CY, Orimo H.** Superoxide anion formation and glutathione metabolism of blood in patients with idiopathic pulmonary fibrosis. *Biochem Mol Med* 55: 66–70, 1995.
46. **Tsao C, Greene P, Odlind B, Brater DC.** Pharmacokinetics of recombinant human superoxide dismutase in healthy volunteers. *Clin Pharmacol Ther* 50: 713–720, 1991.
47. **Walter N, Collard HR, King TE Jr.** Current perspectives on the treatment of idiopathic pulmonary fibrosis. *Proc Am Thorac Soc* 3: 330–338, 2006.
48. **Willis BC, Borok Z.** TGF-β-induced EMT: mechanisms and implications for fibrotic lung disease. *Am J Physiol Lung Cell Mol Physiol* 293: L525–L534, 2007.
49. **Woessner JF Jr.** The determination of hydroxyproline in tissue and protein samples containing small proportions of this imino acid. *Arch Biochem Biophys* 93: 440–447, 1961.
50. **Yamazaki C, Hoshino J, Hori Y, Sekiguchi T, Miyauchi S, Mizuno S, Horie K.** Effect of lecithinized-superoxide dismutase on the interstitial pneumonia model induced by bleomycin in mice. *Jpn J Pharmacol* 75: 97–100, 1997.
51. **Yasui K, Baba A.** Therapeutic potential of superoxide dismutase (SOD) for resolution of inflammation. *Inflamm Res* 55: 359–363, 2006.
52. **Zhao J, Shi W, Wang YL, Chen H, Bringas P Jr, Datto MB, Frederick JP, Wang XF, Warburton D.** Smad3 deficiency attenuates bleomycin-induced pulmonary fibrosis in mice. *Am J Physiol Lung Cell Mol Physiol* 282: L585–L593, 2002.
53. **Zheng J, Jia Y, Zhou K.** A study on enzymatic activities of bronchoalveolar lavage fluid in patients with interstitial lung diseases. *Zhonghua Jie He He Hu Xi Za Zhi* 21: 91–93, 1998.

Biochemical Pharmacology 79 (2010) 1622–1633

Contents lists available at ScienceDirect

Biochemical Pharmacology

journal homepage: www.elsevier.com/locate/biochempharm

Protective effect of rebamipide against celecoxib-induced gastric mucosal cell apoptosis

Tomoaki Ishihara, Ken-Ichiro Tanaka, Saki Tashiro, Kosuke Yoshida, Tohru Mizushima *

Graduate School of Medical and Pharmaceutical Sciences, Kumamoto University, 5-1 Oe-honmachi, Kumamoto 862-0973, Japan

ARTICLE INFO

Article history:
Received 3 December 2009
Accepted 25 January 2010

Keywords:
Celecoxib
Rebamipide
Ulcer
Apoptosis
Voltage-dependent L-type Ca^{2+} channel

ABSTRACT

A major clinical problem encountered with the use of non-steroidal anti-inflammatory drugs (NSAIDs) is gastrointestinal complications. We have previously suggested that both decreases in prostaglandin E_2 (PGE_2) levels and mucosal apoptosis are involved in the development of NSAID-produced gastric lesions and that this apoptosis is mediated by an increase in the intracellular Ca^{2+} concentration and the resulting endoplasmic reticulum (ER) stress response and mitochondrial dysfunction. Celecoxib and rebamipide are being used clinically as a safer NSAID and an anti-ulcer drug, respectively. In this study, we have examined the effect of rebamipide on celecoxib-induced production of gastric lesions. In mice pre-administered with a low dose of indomethacin, orally administered rebamipide suppressed celecoxib-induced mucosal apoptosis and lesion production but did not decrease in PGE_2 levels in the stomach. Rebamipide also suppressed celecoxib-induced increases in intracellular Ca^{2+} concentration, the ER stress response, mitochondrial dysfunction and apoptosis *in vitro*. We also found that rebamipide suppresses the increases in intracellular Ca^{2+} concentration induced by an activator of voltage-dependent L-type Ca^{2+} channels and that another blocker of this channel suppresses celecoxib-induced increases in intracellular Ca^{2+} concentration. These results suggest that celecoxib activates voltage-dependent L-type Ca^{2+} channels and that rebamipide blocks this activation, resulting in suppression of celecoxib-induced apoptosis. We believe that this novel activity of rebamipide may play an important role in the protection of gastric mucosa against the formation of celecoxib-induced lesions.

1. Introduction

Non-steroidal anti-inflammatory drugs (NSAIDs) are a useful family of therapeutics, accounting for nearly 5% of all prescribed medications [1]. An inhibitory effect of NSAIDs on cyclooxygenase (COX) activity is responsible for their anti-inflammatory actions because COX is an enzyme essential for the synthesis of prostaglandins (PGs), such as PGE_2, which have a strong capacity to induce inflammation. On the other hand, NSAID use is associated with gastrointestinal complications, with about 15–30% of chronic users of NSAIDs suffering from gastrointestinal ulcers and bleeding [2–6]. Therefore, establishment of a clinical protocol to treat NSAID-induced gastrointestinal lesions is important.

There are at least two subtypes of COX, COX-1 and COX-2, which are responsible for the majority of COX activity at the gastric mucosa and in inflamed tissues, respectively [7,8]. Therefore, it is reasonable to speculate that selective COX-2 inhibitors could have anti-inflammatory activity without gastrointestinal side effects [7]. In fact, a greatly reduced incidence of acute gastroduodenal lesions has been reported for COX-2-selective inhibitors, such as celecoxib, both in animal and clinical studies [9–12] and thus, celecoxib is used widely in Western countries and recently has become available in Japan. However, the superiority of celecoxib to non-selective NSAIDs in limiting gastric side effects is not as clear in patients taking aspirin concomitantly or in patients using such NSAIDs for a long period [10,13,14]. Therefore, use of COX-2-selective inhibitors does not completely avoid the gastric side effects of NSAIDs and it is important that a clinical protocol to treat celecoxib-induced gastric lesions be established.

Although PGE_2 has a strong protective effect on gastrointestinal mucosa, the inhibition of COX by NSAIDs is not the sole explanation for the gastrointestinal side effects of NSAIDs [15,16]. We have recently demonstrated that NSAIDs induce apoptosis in cultured gastric cells and at gastric mucosa in a manner that is independent of COX inhibition [17–21]. NSAIDs, including celecoxib, increase the intracellular Ca^{2+} concentration [$Ca^{2+}{}_i$]. Using the intracellular Ca^{2+} chelator 1,2-bis(2-aminophenoxy)ethane-N,N,N′N′-tetraacetic acid (BAPTA-AM), we have found evidence that this increase is responsible for NSAID-induced apoptosis [17]. This increase in [Ca^{2+}]$_i$ seems to induce the endoplasmic reticulum (ER) stress response, in which an apoptosis-inducing transcription factor, C/EBP homologous transcription

* *Corresponding author.* Tel.: +81 96 371 4323; fax: +81 96 371 4323.
E-mail address: mizu@gpo.kumamoto-u.ac.jp (T. Mizushima).

0006-2952/$ – see front matter © 2010 Elsevier Inc. All rights reserved.
doi:10.1016/j.bcp.2010.01.030

factor (*chop*), is induced and we have previously shown, *chop* is essential for NSAID-induced apoptosis [18]. With the aid of activating transcription factor 4 (*atf4*), *chop* induces expression of p53 up-regulated modulator of apoptosis (*puma*) and the resulting activation of Bax [22]. We have already shown that both *puma* and Bax play important roles in NSAID-induced mitochondrial dysfunction, activation of caspases and apoptosis [17,22–24]. Furthermore, we have suggested that both COX inhibition (resulting in a decrease in gastric PGE_2 levels) and gastric mucosal apoptosis are required for the formation of NSAID-induced gastric lesions *in vivo* [21,25,26]. Therefore, it will be important to consider protection of gastric mucosal cells against celecoxib-induced apoptosis when establishing a clinical protocol to treat celecoxib-induced gastric lesions.

Rebamipide is an anti-ulcer drug used in Asian countries [27,28]. Both animal and clinical studies have revealed that rebamipide prevents the formation of NSAID-induced gastric lesions [27–30]; however, no clinical or animal data regarding the effect of rebamipide on celecoxib-induced gastric lesions have been reported. Rebamipide has various gastroprotective mechanisms, such as decreasing reactive oxygen species (ROS) and up-regulating COX-2 expression; this latter function increases gastric PGE_2 levels, which in turn stimulates mucus secretion and gastric mucosal blood flow [27,31–33]. Furthermore, the protective effect of rebamipide on cells against indomethacin-induced apoptosis has been reported *in vitro* [34,35]. However, the effect of rebamipide on celecoxib-induced apoptosis has not been reported. In this study, we have obtained *in vivo* data suggesting that orally administered rebamipide suppresses the formation of celecoxib-produced gastric lesions through suppression of mucosal apoptosis. It was also found that rebamipide suppresses the celecoxib-induced increase in $[Ca^{2+}]_i$, the ER stress response, mitochondrial dysfunction and apoptosis *in vitro*. We suggest that rebamipide achieves these effects through inhibition of a voltage-dependent L-type Ca^{2+} channel.

2. Materials and methods

2.1. Chemicals and animals

RPMI 1640 was obtained from Nissui Pharmaceutical Co (Osaka, Japan). Rebamipide was kindly provided by Otsuka Pharmaceutical Co (Tokushima, Japan). Pluronic F127, fluo-3/AM, 4′, 6-diamidino-2-phenylindole dihydrochloride (DAPI) and BAPTA-AM were obtained from Dojindo Co (Kumamoto, Japan). Paraformaldehyde, fetal bovine serum (FBS), tunicamycin, thapsigargin, ionomycin, Hoechst 33258 and (S)-(-)-BAY K 8644 (BAYK 8644) were obtained from Sigma (St. Louis, MO). Indomethacin, ibuprofen, diclofenac and nifedipine were obtained from Wako Co (Osaka, Japan). Celecoxib was from LKT Laboratories Inc (St Paul, MN). A PGE_2 enzyme immuno assay (EIA) kit was purchased from Cayman Chemical (Ann Arbor, MI). Antibodies against *puma* or the N-terminal region of Bax (Bax N20) and actin were purchased from ProSci Inc (Poway, CA) or Santa Cruz Biotechnology (Santa Cruz, CA), respectively. An antibody against cytochrome *c* was from PharMingen (San Jose, CA). Terminal deoxynucleotidyl transferase (TdT) was obtained from TOYOBO (Osaka, Japan). Mayer's hematoxylin, 1% eosin alcohol solution and mounting medium for histological examination (Malinol) were from MUTO Pure Chemicals (Tokyo, Japan). Biotin 14-ATP, Alexa Fluor 488 goat anti-rabbit immunoglobulin G and Alexa Fluor 488 conjugated with streptavidin were purchased from Invitrogen (Carlsbad, CA). Mounting medium (VECTASHIELD) was from Vector Laboratories (Burlingame, CA). The RNeasy kit was obtained from QIAGEN (Valencia, CA), the first-strand cDNA synthesis kit was from Takara (Kyoto, Japan), and iQ SYBR Green Supermix was from Bio-Rad (Hercules, CA). Wild-type mice (C57/BL6) (8–10 weeks of age and 25 to 30 g) were used. The experiments and procedures described here were carried out in accordance with the Guide for the Care and Use of Laboratory Animals as adopted and promulgated by the National Institutes of Health (Bethesda, MD) and were approved by the Animal Care Committee of Kumamoto University.

2.2. Gastric damage assay

The gastric ulcerogenic response was examined as described previously [25], with some modifications. Mice fasted for 18 h were intravenously administered indomethacin in PBS via the tail vein and 1 h later, orally administered celecoxib in 1% methylcellulose in a volume of 10 ml/kg. In some experiments, mice were orally administered rebamipide in 0.5% carboxymethylcellulose in a volume of 10 ml/kg 1 h before the administration of indomethacin. Eight hours after the administration of celecoxib, the animals were sacrificed, after which their stomachs were removed and the areas of the gastric mucosal lesions were measured by an observer unaware of the treatment they had received. Calculation of the scores involved measuring the area of all the lesions in square millimetres and summing the values to give an overall gastric lesion index. The gastric PGE_2 level was determined by EIA according to the manufacturer's instructions.

2.3. Cell culture and assay for apoptosis and K^+ efflux

Human gastric adenocarcinoma (AGS) cells were cultured in RPMI 1640 medium supplemented with 10% FBS, 100 U/ml penicillin and 100 μg/ml streptomycin in a humidified atmosphere of 95% air with 5% CO_2 at 37 °C. Cells were exposed to celecoxib by changing the medium. Cells were cultured for 24 h and then used in experiments. Apoptosis was monitored by fluorescence-activated cell sorting (FACS) analysis, chromatin condensation by staining with Hoechst dye 33258 and caspase-3-like activity as previously described [18,20,23]. K^+ efflux from cells was monitored as previously described [17,36].

2.4. Real-time RT-PCR analysis

Total RNA was extracted from AGS cells using an RNeasy kit according to the manufacturer's protocol. Samples (2.5 μg of RNA) were reverse-transcribed using a first-strand cDNA synthesis kit according to the manufacturer's instructions. Synthesized cDNA was used in real-time RT-PCR (Bio-Rad Chromo 4 system) experiments using iQ SYBR Green Supermix and analysed with Opticon Monitor software according to the manufacturer's instructions. The real-time PCR cycle conditions were 95 °C for 3 min, followed by 44 cycles at 95 °C for 10 s and at 60 °C for 60 s. Specificity was confirmed by electrophoretic analysis of the reaction products and by inclusion of template- or reverse transcriptase-free controls. To normalize the amount of total RNA present in each reaction, actin cDNA was used as an internal standard.

Primers were designed using the Primer3 website (http://frodo.wi.mit.edu/cgi-bin/primer3/primer3_www.cgi). The primers used were (name, forward primer and reverse primer): *atf4*, 5′-tcaaacctcatgggttctcc-3′ and 5′-gtgtcatccaacgtggtcag-3′; *chop*, 5′-tgcctttctcttcggacact-3′ and 5′-tgtgacctctgctggttctg-3′; *puma*, 5′-gacgacctcaacgcacagta-3′ and 5′-ggagtcccatgatgagattgt-3′; *actin*, 5′-tgcctttctcttcggacact-3′ and 5′-tgtgacctctgctggttctg-3′.

2.5. Immunoblotting analysis

Total protein was extracted as described previously [37]. The protein concentration of each sample was determined